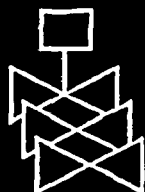
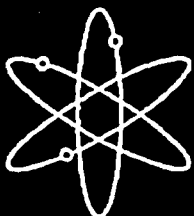
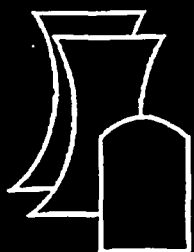


**DORT/TORT Analyses of  
the Hatch Unit-1 Jet Pump Riser  
Brace Pad Neutron Dosimetry  
Measurements with Comparisons  
to Predictions Made with RAMA**

**Brookhaven National Laboratory**

**U.S. Nuclear Regulatory Commission  
Office of Nuclear Regulatory Research  
Washington, DC 20555-0001**



## AVAILABILITY OF REFERENCE MATERIALS IN NRC PUBLICATIONS

### NRC Reference Material

As of November 1999, you may electronically access NUREG-series publications and other NRC records at NRC's Public Electronic Reading Room at <http://www.nrc.gov/reading-rm.html>. Publicly released records include, to name a few, NUREG-series publications; *Federal Register* notices; applicant, licensee, and vendor documents and correspondence; NRC correspondence and internal memoranda; bulletins and information notices; inspection and investigative reports; licensee event reports; and Commission papers and their attachments.

NRC publications in the NUREG series, NRC regulations, and *Title 10, Energy*, in the Code of *Federal Regulations* may also be purchased from one of these two sources.

1. The Superintendent of Documents  
U.S. Government Printing Office  
Mail Stop SSOP  
Washington, DC 20402-0001  
Internet: bookstore.gpo.gov  
Telephone: 202-512-1800  
Fax: 202-512-2250
2. The National Technical Information Service  
Springfield, VA 22161-0002  
[www.ntis.gov](http://www.ntis.gov)  
1-800-553-6847 or, locally, 703-605-6000

A single copy of each NRC draft report for comment is available free, to the extent of supply, upon written request as follows:

Address: Office of the Chief Information Officer,  
Reproduction and Distribution  
Services Section  
U.S. Nuclear Regulatory Commission  
Washington, DC 20555-0001  
E-mail: [DISTRIBUTION@nrc.gov](mailto:DISTRIBUTION@nrc.gov)  
Facsimile: 301-415-2289

Some publications in the NUREG series that are posted at NRC's Web site address <http://www.nrc.gov/reading-rm/doc-collections/nuregs> are updated periodically and may differ from the last printed version. Although references to material found on a Web site bear the date the material was accessed, the material available on the date cited may subsequently be removed from the site.

### Non-NRC Reference Material

Documents available from public and special technical libraries include all open literature items, such as books, journal articles, and transactions, *Federal Register* notices, Federal and State legislation, and congressional reports. Such documents as theses, dissertations, foreign reports and translations, and non-NRC conference proceedings may be purchased from their sponsoring organization.

Copies of industry codes and standards used in a substantive manner in the NRC regulatory process are maintained at—

The NRC Technical Library  
Two White Flint North  
11545 Rockville Pike  
Rockville, MD 20852-2738

These standards are available in the library for reference use by the public. Codes and standards are usually copyrighted and may be purchased from the originating organization or, if they are American National Standards, from—

American National Standards Institute  
11 West 42<sup>nd</sup> Street  
New York, NY 10036-8002  
[www.ansi.org](http://www.ansi.org)  
212-642-4900

Legally binding regulatory requirements are stated only in laws; NRC regulations; licenses, including technical specifications; or orders, not in NUREG-series publications. The views expressed in contractor-prepared publications in this series are not necessarily those of the NRC.

The NUREG series comprises (1) technical and administrative reports and books prepared by the staff (NUREG-XXXX) or agency contractors (NUREG/CR-XXXX), (2) proceedings of conferences (NUREG/CP-XXXX), (3) reports resulting from international agreements (NUREG/IA-XXXX), (4) brochures (NUREG/BR-XXXX), and (5) compilations of legal decisions and orders of the Commission and Atomic and Safety Licensing Boards and of Directors' decisions under Section 2.206 of NRC's regulations (NUREG-0750).

**DISCLAIMER:** This report was prepared as an account of work sponsored by an agency of the U.S. Government. Neither the U.S. Government nor any agency thereof, nor any employee, makes any warranty, expressed or implied, or assumes any legal liability or responsibility for any third party's use, or the results of such use, of any information, apparatus, product, or process disclosed in this publication, or represents that its use by such third party would not infringe privately owned rights.

NUREG/CR-6887  
BNL-NUREG-75098-2005

---

---

# **DORT/TORT Analyses of the Hatch Unit-1 Jet Pump Riser Brace Pad Neutron Dosimetry Measurements with Comparisons to Predictions Made with RAMA**

---

---

Manuscript Completed: April 2004  
Date Published: November 2005

Prepared by  
J.F. Carew, K. Hu, A. Aronson,  
A.N. Mallen and M. Todosow

Brookhaven National Laboratory  
Upton, NY 11973-5000

With contributions by  
D.B. Jones and K.E. Watkins

TransWare Enterprises, Inc.

W.E. Norris, NRC Project Manager

Prepared for  
Division of Engineering Technology  
U.S. Nuclear Regulatory Commission  
Washington, DC 20555-0001  
NRC Job Code Y6883



## ABSTRACT

Regulatory Guide 1.190 for determining pressure vessel fast neutron fluence requires that the vessel fluence calculational methodology be evaluated using dosimetry measurement benchmarks. To insure the viability of the underwater welding that has been proposed for repairing Boiling Water Reactor (BWR) highly irradiated stainless and high nickel alloy vessel internals, an accurate and well benchmarked calculational method is required for determining the BWR thermal fluence. The recent Electric Power Research Institute (EPRI)/ Nuclear Regulatory Commission (NRC) measurement program performed at Hatch-1 provides both a fast and thermal neutron dosimetry data-base for benchmarking BWR fluence calculation methodologies.

Under the NRC "BWR Fluence" Program (JCN-Y-6391), the neutron dosimetry measurements performed at Hatch-1 are being used as a data base for assessing the accuracy of calculational methodologies used to predict neutron fluence accumulated by BWR internal components and the vessel. Results from both the well established DORT/TORT computer codes and the new state-of-the-art RAMA Fluence Methodology were to be compared in order to reduce the uncertainty in fluence estimates, and in the future, to permit a better evaluation of the feasibility of underwater welding techniques of highly irradiated components.

Detailed calculations of the Hatch-1 jet pump riser brace pad thermal and fast neutron dosimetry measurements have been performed by Brookhaven National Laboratory (BNL) using the DORT/TORT discrete ordinates transport methodology and by Transware Enterprises Inc. (TWE) using the RAMA three-dimensional fluence methodology. The calculations for both code models were performed using nuclear data primarily based on the BUGLE-96 nuclear data library. The calculations were performed using a detailed description of the Hatch-1 core/internals/vessel material and geometrical configuration. The core neutron source includes the effects of the pin-wise power distribution on the core periphery and the effects of plutonium buildup on the magnitude and energy dependence of the neutron source.

Comparisons of the fluences calculated by DORT/TORT (performed by BNL), and fluences and activations calculated by RAMA (performed by TWE), and the Hatch-1 measurements have been performed to assess the accuracy of the methodologies for predicting the fast and thermal neutron fluence of BWR internal components and the vessel. Measurement-to-Calculation (M/C) fluence comparisons were also performed. The DORT/TORT methodology was found to predict the fast and thermal fluence measurements to within ~ 5% and ~15%, respectively. The DORT/TORT fluence measurement predictions by BNL are considered to be within the combined accuracy of the calculations and measurements. The DORT/TORT thermal fluence calculations showed an average measurement to calculation ratio of 1.17. The DORT/TORT calculation under-predicted the thermal fluence measurement by ~15%.

The RAMA methodology by TWE was found to predict the fast fluence measurements to within ~ 7%. The thermal fluence measurements were predicted by RAMA with a measurement to calculation ratio of ~0.62 with a standard deviation of 0.2%. The RAMA methodology performs a direct three-dimensional solution of the transport equation and calculates fluence predictions. The fast predictions are in good agreement with measurements. However, the RAMA code over-predicted the measured thermal fluence by ~60%. The agreement between calculated and measured fast and thermal activations was similar to that of the fluence in both direction and magnitude. The large difference between the RAMA calculated thermal fluence and the measured thermal fluence at the pressure vessel wall warrants further investigation.

The DORT/TORT-to-RAMA differences for the fast fluence measurements are ~4%, and are consistent with the accuracy of the two calculational methods. The large over-prediction (~60%) in the RAMA thermal fluence, compared to the measured fluence, prevents any meaningful comparison with the DORT/TORT synthesis approach at BNL. The DORT/TORT approach under-predicted the thermal fluence measurements by an average of ~15%.

# CONTENTS

Page

Abstract .....	iii
List of Figures .....	vi
List of Tables .....	vii
Foreword .....	ix
Acknowledgments .....	xi
1 Introduction .....	1-1
2 Hatch-1 Riser Brace Pad Dosimetry Measurements .....	2-1
3 Hatch-1 Plant Data .....	3-1
3.1 Introduction .....	3-1
3.2 Core, Internals and Vessel Geometry and Materials Data .....	3-1
3.3 Jet Pump Riser Brace Pad Geometry and Materials Data .....	3-2
3.4 Core Neutron Source Data .....	3-2
4 Calculational Methods .....	4-1
4.1 Introduction .....	4-1
4.2 Neutron Cross Sections and Fission Spectra .....	4-1
4.2.1 DORT/TORT Fission Spectra .....	4-1
4.2.2 RAMA Fission Spectra .....	4-1
4.3 Core Neutron Source .....	4-1
4.3.1 DORT/TORT Source Calculation .....	4-1
4.3.2 RAMA Source Calculation .....	4-2
4.4 DORT/TORT Neutron Transport Calculations .....	4-2
4.4.1 Neutron Transport Method .....	4-2
4.4.2 Flux Synthesis Method .....	4-2
4.4.3 Dosimetry Cross Sections .....	4-3
4.4.4 Thermal Fluence Calculation .....	4-3
4.4.5 TORT Calculations of the Effect of the Local Brace Pad Geometry .....	4-3
4.5 RAMA Neutron Transport Calculations .....	4-4
4.5.1 Neutron Transport Method .....	4-4
4.5.2 The RAMA Fluence Model .....	4-4
4.5.3 Dosimetry Cross Sections .....	4-5
4.5.4 Thermal Fluence Calculation .....	4-5
5 Comparisons of Calculations and Measurements .....	5-1
5.1 Introduction .....	5-1
5.2 Brace Pad Dosimetry and Fluence Comparisons .....	5-1
5.2.1 Comparison of Fluence Calculations with Measurement .....	5-1
5.2.2 Comparison of DORT/TORT and RAMA Fluence Results .....	5-1
5.2.3 Comparison of RAMA Activity Calculations With Measurements .....	5-2
6 Summary and Conclusion .....	6-1
7 References .....	7-1

## FIGURES

	Page
2.1	Hatch-1 Jet Pump and Riser Assembly ..... 2-3
2.2	Hatch-1 Jet Pump Riser and Brace ..... 2-4
2.3	Azimuthal Locations of Hatch-1 Riser Brace Pad Dosimetry Measurements ..... 2-5
2.4	Location of Hatch-1 Brace Pad Dosimetry Samples Viewed from Inside the Vessel ..... 2-6
3.2.1	Hatch-1 Fuel Assembly Lattice Geometry ..... 3-8
3.2.2	Hatch-1 Core Configuration ..... 3-9
3.2.3	Radial Fuel Assembly Material Groups ..... 3-10
3.3.1	Hatch-1 Jet Pump Riser and Brace Configuration ..... 3-11
3.3.2	Azimuthal Location of Jet Pump Riser Brace Pad on Pressure Vessel ..... 3-12
3.3.3	Horizontal View of Jet Pump Riser Brace Pad ..... 3-13
3.3.4	Horizontal and Vertical View of Jet Pump Riser Brace ..... 3-14
3.3.5	Vertical View of Jet Pump Riser Brace ..... 3-15
4.1	Hatch-1 Planar Geometry. .... 4-7
4.2	Hatch-1 Axial Geometry ..... 4-8
4.3	Top View of the Hatch-1 TORT Riser and Brace Model. .... 4-9
4.4	Side View of the Hatch-1 TORT Riser and Brace Model ..... 4-10
4.5	Horizontal View of the Hatch-1 TORT Riser and Brace Model ..... 4-11
4.6	Top View of the Hatch-1 RAMA Model Near the Jet Pump Riser Brace Assembly Elevation ..... 4-12
4.7	Axial View of the Hatch-1 RAMA Jet Pump Riser Brace Assembly Model ..... 4-13
4.8	Front View of the Hatch-1 RAMA Jet Pump Riser Brace Pad ..... 4-14

# TABLES

	Page
2.1 Hatch-1 Brace Pad Fast and Thermal Fluence Measured Reaction Rates .....	2-2
3.2.1 Hatch-1 Core/Internals/Vessel Geometry and Materials Data .....	3-3
3.2.2 Cycle 1-4 Core Material Compositions .....	3-4
3.2.3 Cycle 5-12 Core Material Compositions .....	3-5
3.2.4 Cycle 13-19 Core Material Compositions .....	3-6
3.2.5 Vessel and Internals Material Compositions .....	3-7
4.2.1 Fraction of Fissions by Isotope as a Function of Fuel Exposure .....	4-6
4.2.2 TORT Calculations of the Effect of the Riser Brace and Brace Pad on the Dosimetry Measurements ...	4-6
5.2.1 Comparison of the Jet Pump-3 and 13 Measured and DORT/TORT Calculated Fluences .....	5-3
5.2.2 Comparison of the Jet Pump-5 and 15 Measured and DORT/TORT Calculated Fluences .....	5-3
5.2.3 Comparison of the Jet Pump-3 and 13 Measured and RAMA Calculated Fluences .....	5-4
5.2.4 Comparison of the Jet Pump-5 and 15 Measured and RAMA Calculated Fluences .....	5-4
5.2.5 Comparison of the DORT/TORT and RAMA Predictions of the Jet Pump-3 and 13 Measurements ....	5-5
5.2.6 Comparison of the DORT/TORT and RAMA Predictions of the Jet Pump-5 and 15 Measurements ....	5-5
5.2.7 Comparison of Jet Pump-3 and 13 Activation Measurements ( $\mu\text{Ci}/\text{mg}$ ) to RAMA Calculated Activations	5-6
5.2.8 Comparison of Jet Pump-5 and 15 Activation Measurements ( $\mu\text{Ci}/\text{mg}$ ) to RAMA Calculated Activations	5-7
5.2.9 Comparison of the Activation Measurements to RAMA Calculated Activities .....	5-7

## FOREWORD

Industry operating experience has demonstrated the occurrence of cracking in stainless steel and high Nickel alloy core internal components of boiling water reactors (BWRs), and the incidence of cracking is expected to increase as U.S. nuclear power plants continue to age. To address this issue, the Electric Power Research Institute (EPRI) is studying a variety of repair and mitigation strategies. Mechanical repairs are not always practical because of obstructions. As a result, for many components, welded repairs may be the only viable strategy. For irradiated stainless steels, however, welded repairs may not be viable due to the potential for cracking.

The issue at hand is that Helium, which is produced in stainless steel components as a result of irradiation, accumulates during welding and forms bubbles that grow rapidly, and these bubbles can lead to cracking during the welding process. Helium results from the transmutation of Boron and Nickel; however, the Boron content of U.S. BWR components is usually unknown because Boron is an impurity in stainless steels.

EPRI began gathering information in the late 1990s concerning the feasibility of welding stainless steels with varying Helium content. However, EPRI soon determined that additional information would be needed in order to render a sound technical judgment concerning the acceptability of such welding for BWRs in the United States.

The U.S. Nuclear Regulatory Commission (NRC) and EPRI signed a cooperative agreement on January 11, 2000, to address the cracking of stainless steel and high Nickel alloy in-vessel components of U.S. BWRs. Research conducted under that agreement has identified Helium content thresholds to ensure acceptable weldability of highly irradiated stainless steels.

Helium content can be determined through measurement or estimated by analytical methods. The most reliable method is measurement where very small samples are removed from the components of interest to measure their respective Helium content. However, sampling and measurement are costly and time-consuming. Analytical methods (computer codes) can be used to calculate Helium content provided that the fluence of the given material (a measure of the number of neutrons striking the material) is known. Prior to this study, the fluence had not yet been assessed for many of the components of interest. Small samples were taken by Framatome ANP from typical BWR jet pump riser brace pads (JPRBPs). The samples were analyzed by Pacific Northwest National Laboratory (PNNL) for Helium content, initial Boron content, and accumulated fluence.

The NRC staff has relied for many years on the well established DORT/TORT computer code for calculating pressure vessel fluence. However, modeling the complex three-dimensional geometry of in-vessel components is difficult using DORT/TORT. In addition, the code had been benchmarked only for the estimation of fast neutron (high-energy) fluence. Epithermal and resonance thermal neutron capture is also required to accurately calculate the concentration of Helium. Independently, EPRI had previously sponsored TransWare Enterprises Inc. (TWE) to develop a new, state-of-the-art three-dimensional computer code, known as RAMA to estimate fast and thermal neutron fluence. This information could then be used for comparisons with estimates from analytical methods.

During the course of their cooperative effort, the NRC and EPRI discussed the need to compare the laboratory-measured fluence (from the work at PNNL) to those calculated by the DORT/TORT (BNL) and RAMA (TWE) codes.



The study originally intended to evaluate how well the DORT/TORT and RAMA transport codes estimated the fast and thermal neutron fluences of the JPRBPs compared to the laboratory-measured values of the actual samples. The fast fluence evaluations were completed, but shortly after the thermal fluence comparison efforts were initiated, several high priority emerging issues compelled a re-evaluation of research activities. The thermal fluence evaluations were initiated but not fully completed. The code comparisons indicated that, for the specific comparisons made, the fast neutron fluences ( $E > 1.0$  MeV) calculated using both the DORT/TORT and RAMA codes agree well with the laboratory-measured values of the actual samples. Specifically, DORT/TORT predicted fast fluence to within approximately 5 percent of the laboratory-measured values of the actual samples, and RAMA predicted fast fluence to within approximately 7 percent, which is within the uncertainties of the two calculational methods. The thermal fluence calculations, however, did not show the same consistency. Rather, the DORT/TORT code *underpredicted* thermal fluence relative to the laboratory-measured values of the actual samples by approximately 15 percent on average, while the RAMA code *overpredicted* thermal fluence by approximately 60 percent. This was a first attempt at benchmarking thermal fluence, and the causes of the discrepancies are not understood at this time. Therefore, the industry has initiated additional investigation into the source of the discrepancies in the thermal fluence calculations.

The cooperative research described in this report describes preliminary efforts to estimate the Helium content and fluences of irradiated stainless steels through the use of computer codes. Although work was terminated before completion, the preliminary results provide a starting point for further analysis in efforts to use computer codes in lieu of sampling in-vessel components to make weldability determinations.



---

Carl J. Paperiello, Director  
Office of Nuclear Regulatory Research  
U.S. Nuclear Regulatory Commission

## **ACKNOWLEDGMENTS**

The work documented in this report was performed under the auspices of the United States Nuclear Regulatory Commission (USNRC). It was funded by the Materials Engineering Branch of the Division of Engineering Technology in the Office of Nuclear Regulatory Research, under Job Code JCN Y-6883. The program was monitored at the USNRC by W. E. Norris whose support of this work is greatly appreciated. The authors are also grateful to Nilesh Chokshi and Michael Mayfield of the Office of Nuclear Regulatory Research for many valuable discussions and contributions to this work.

The authors would like to thank the Southern Nuclear Operating Company staff for their cooperation and support in providing the detailed Hatch-1 plant data required for this evaluation, especially Nancy Folk, Kenneth Folk, Robin Dyle and Marty Sims. The cooperation of Dean Jones and Kenneth Watkins of TransWare Enterprises Inc., and Kenneth Wolfe and Robert Carter of the Electric Power Research Institute is also greatly appreciated.

TransWare Enterprises Inc. (TWE) performed all the RAMA calculations and provided the RAMA results used in this report under a subcontract to Brookhaven National Laboratory (BNL).

# 1 INTRODUCTION

The fracture toughness of light water reactor pressure vessel materials is measured in terms of the Reference Temperature for nil-ductility transition ( $RT_{NDT}$ ). The  $RT_{NDT}$  is defined as a function of the material chemistry (concentration of Cu and Ni) and the fast neutron ( $>1$  MeV) vessel fluence. Because of the limited margin between the predicted and limiting value of  $RT_{NDT}$  at certain plants and in order to provide the necessary confidence in the fracture toughness and integrity of the reactor pressure vessel, an accurate calculation of the vessel  $>1$  MeV fluence is required.

In addition, underwater welding has been proposed as a means of repairing BWR stainless and high nickel alloy vessel internals that have experienced environmentally assisted cracking (Reference-1). However, the feasibility of the underwater welding of highly irradiated components is dependent on the concentration of He present in the steel due to thermal neutron capture in trace amounts of B-10 and Ni-58 present in the original material.<sup>1</sup> Consequently, in order to determine the He concentration and insure the viability of the proposed welds, an accurate estimate of the neutron fluence accumulated by the vessel internals is required.

Because of the several decades of attenuation in the neutron flux between the core and the pressure vessel, the vessel fluence calculation is extremely sensitive to the material and geometrical representation, the nuclear cross section data, and the numerical schemes used in its determination. These factors combine to make an accurate calculation of the internal components and vessel fluence difficult. To provide the necessary level of confidence in the vessel fluence predictions, Regulatory Guide 1.190 for determining pressure vessel neutron fluence (Reference-2) requires that the vessel fluence calculational methodology be evaluated using dosimetry measurement benchmarks.

As part of the work being performed under an Addendum to an NRC/EPRI Memorandum of Understanding (MOU), material samples from several operating BWRs have been removed and characterized. The characterization of these samples includes: (1)

---

<sup>1</sup>The He producing reactions are:  
(1)  $B^{10} + n \rightarrow Li^7 + \alpha$  and (2)  $Ni^{58} + n \rightarrow Ni^{59} + \gamma$ ,  
 $Ni^{59} + n \rightarrow Fe^{56} + \alpha$ .

dosimetry activations and the determination of thermal and fast neutron fluence (Reference-3a and Reference-3b) and (2) helium and boron concentrations of scrapings from the jet pump riser brace pads located on the vessel inner wall (Reference-3a). Under the NRC "Boiling Water Reactor (BWR) Fluence Program (JCN Y-6391)," these measurements are being used to provide a dosimetry data-base for benchmarking calculation methodologies used to predict the fluence accumulated by the BWR internal components and vessel.

This report documents the DORT/TORT Fluence Methodology calculations performed by Brookhaven National Laboratory (BNL) and the RAMA Fluence Methodology calculations performed by TransWare Enterprises Inc. (TWE) of the Hatch-1 dosimetry measurements. The DORT/TORT discrete ordinates transport code system used at BNL represents a well established methodology used for radiation transport computation. The DORT/TORT code system was developed by the Oak Ridge National Laboratory (ORNL) (Reference-4). The RAMA Fluence Methodology (RAMA) that was used by TWE represents a new state-of-the-art methodology for fluence determination (Reference-5). RAMA was developed by TransWare Enterprises Inc. (TWE) under sponsorship of the Electric Power Research Institute (EPRI) and the Boiling Water Reactor Vessel and Internals Project (BWRVIP).

The purpose of the comparisons of the DORT/TORT and the RAMA fluence calculations was to compare the uncertainties in fluence estimates, allow the evaluation of a more modern computer code, and improve and advance the state of knowledge in the area of radiation transport computation. The calculations were performed using a detailed description of the Hatch-1 core/internals/vessel material and geometrical configuration provided by the Licensee, Southern Nuclear Operating Company. In order to insure an accurate calculation, a substantial effort was made to determine the core neutron source through Cycle-19 when the brace pad scrapings were taken. The neutron source is based on the Hatch-1 three-dimensional power and exposure distributions, and pin-wise power distributions for the fuel bundles close to the core boundary. The neutron source was based on plant Process Computer data for cycles 1-12, and on plant nodal calculations for cycles 13-19.

The present analysis differs from traditional vessel fluence evaluations in two respects. First, the present analysis requires the determination of the neutron thermal reaction rates and fluences whereas typical vessel analyses focus primarily on the  $>1$  MeV and  $>0.1$  MeV fluences. Second, because the relatively complex local geometry involving the riser, brace yoke and leaves surrounding the brace pads has a substantial three-dimensional character, special consideration was required to insure accurate estimates of the fluence at the brace pads.

The Hatch-1 jet pump riser brace pad dosimetry measurements are described in Section-2. The Hatch-1 plant data including: (1) the core/internals/vessel material and geometrical configuration and (2) the core neutron source are given in Section-3. The DORT/TORT and RAMA calculational methods used to predict the brace pad measurements are described in Section-4. The measurement-to-calculation ratios for the DORT/TORT and RAMA methods, and the DORT/TORT-to-RAMA fluence comparisons are presented in Section-5. A summary of the results, and the conclusions, are presented in Section-6.

## 2 HATCH-1 RISER BRACE PAD DOSIMETRY MEASUREMENTS

The Hatch-1 jet pump riser brace pad (JPRBP) measurements were made, in part, to provide a fast and thermal neutron dosimetry data base for an operating BWR plant. The samples were taken by Framatome Technologies after the Cycle-19 shutdown on September 30, 2000. The samples consisted of small "divots" drilled from the inside surface of the Inconel-182 brace pads to a depth of 0.1524 cm. The divots were drilled from a location in the brace pads located immediately to the right (viewed from inside the vessel) of Jet Pumps 3, 5, 13 and 15. (Note: The Jet Pumps described here are also referred to as mixer tubes in this report.) The specific location of the samples is shown in Figures 2.1-2.4. As shown in Figure-2.4, the samples were taken from the left-hand side (viewed from inside the vessel) of the brace pad. It is noteworthy that Jet Pump-3 and Jet Pump-13 are at azimuthally-symmetric locations and, except for differences between the design and as-built plant configuration, should yield identical results. Jet Pump-5 and Jet Pump-15 are also at azimuthally-symmetric locations.

The  $>1$  MeV,  $>0.1$  MeV and thermal fluence for the brace pad dosimetry samples at each of the four jet pump locations were determined from the measured activities for the reaction rates given in Table-2.1 (taken from Reference-3a). The  $>1$  MeV and  $>0.1$  MeV fast neutron fluences are based on measurements of the Fe-54 (n, p) Mn-54, Ni-58 (n, p) Co-58 and Nb-93 (n, n') Nb-93m residual gamma activities. The thermal neutron fluence estimates are based on measurements of the gamma activities associated with the Fe-54 (n,  $\gamma$ ) Fe-55, Ni-62 (n,  $\gamma$ ) Ni-63, Fe-58 (n,  $\gamma$ ) Fe-59, Cr-50 (n,  $\gamma$ ) Cr-51 and Co-59 (n,  $\gamma$ ) Co-60 reactions. The samples were gamma counted and then adjusted to the Hatch-1 initial full power (2436 MW) using the plant operating history.<sup>2</sup> The activities were adjusted to account for reaction product decay during plant operation and up to the time of counting. Corrections were made for gamma self-absorption and interfering reactions. However, because the samples were taken from the surface of the brace pad, the fluence did not require an adjustment for the effects of neutron self-absorption. Adjustments for burnup and transmutation of target and product isotopes were also

considered unnecessary because of the relatively low fluence at the vessel. The thermal activities were reduced to account for the contribution from epithermal absorption.

The fluence estimates inferred from these activities include adjustments for isotope decay, interfering reactions and epithermal absorption. When the fluence estimates for the individual reaction rates are combined, the one-sigma fluence uncertainty due to the measurement is  $\sim 10\%$ . However, in view of the relatively large ( $\sim 30\%$  in the case of the thermal measurements) asymmetries observed between symmetric locations, the total measurement uncertainty, for both fast and thermal fluence, is believed to be somewhat larger (especially for the thermal fluence)  $\sim 10-15\%$ .

---

<sup>2</sup>The gamma counting and processing were performed by L. R. Greenwood and are described in detail in Reference-3a.

Table 2.1 - Hatch-1 Brace Pad Fast and Thermal Fluence Measured Reaction Rates.

Thermal	Fast > 0.1-MeV	Fast > 1-MeV
$^{54}\text{Fe}(n, \gamma)^{55}\text{Fe}$	$^{93}\text{Nb}(n, n')^{93\text{m}}\text{Nb}$	$^{93}\text{Nb}(n, n')^{93\text{m}}\text{Nb}$
$^{62}\text{Ni}(n, \gamma)^{63}\text{Ni}$	$^{54}\text{Fe}(n, p)^{54}\text{Mn}$	$^{54}\text{Fe}(n, p)^{54}\text{Mn}$
$^{58}\text{Fe}(n, \gamma)^{59}\text{Fe}$	$^{58}\text{Ni}(n, p)^{58}\text{Co}$	$^{58}\text{Ni}(n, p)^{58}\text{Co}$
$^{50}\text{Cr}(n, \gamma)^{51}\text{Cr}$		
$^{59}\text{Co}(n, \gamma)^{60}\text{Co}$		

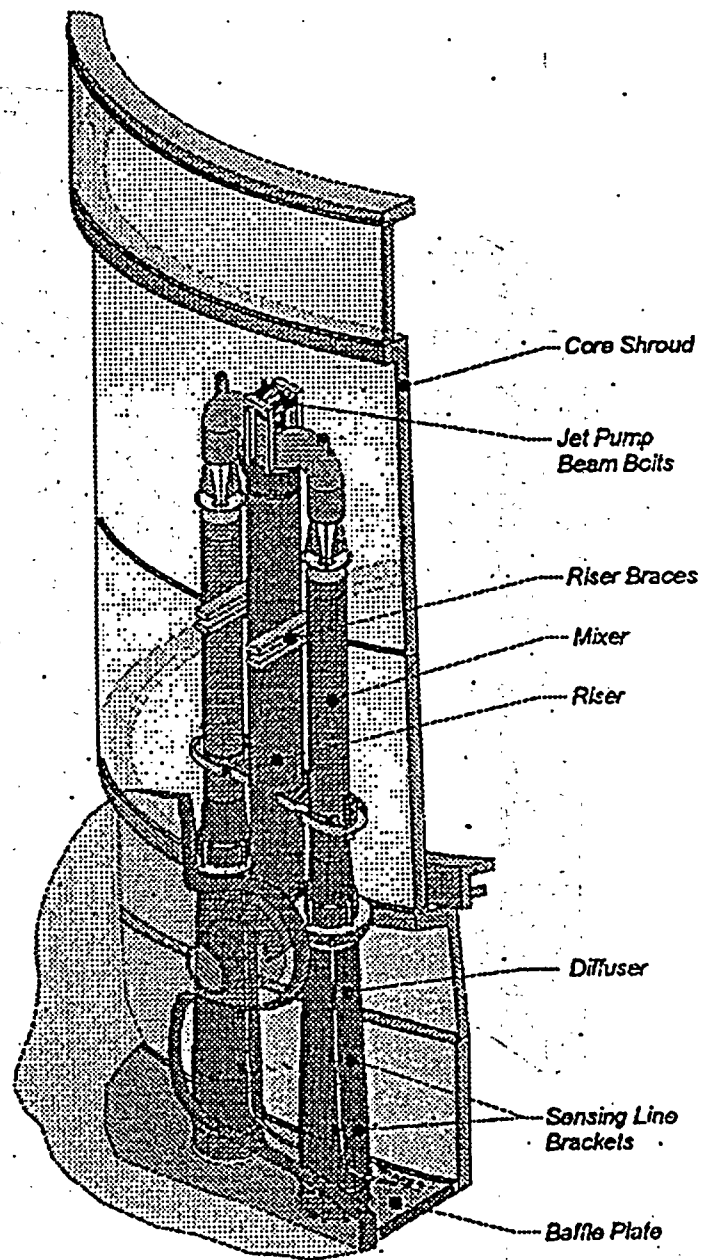


Figure 2.1. Hatch-1 Jet Pump and Riser Assembly

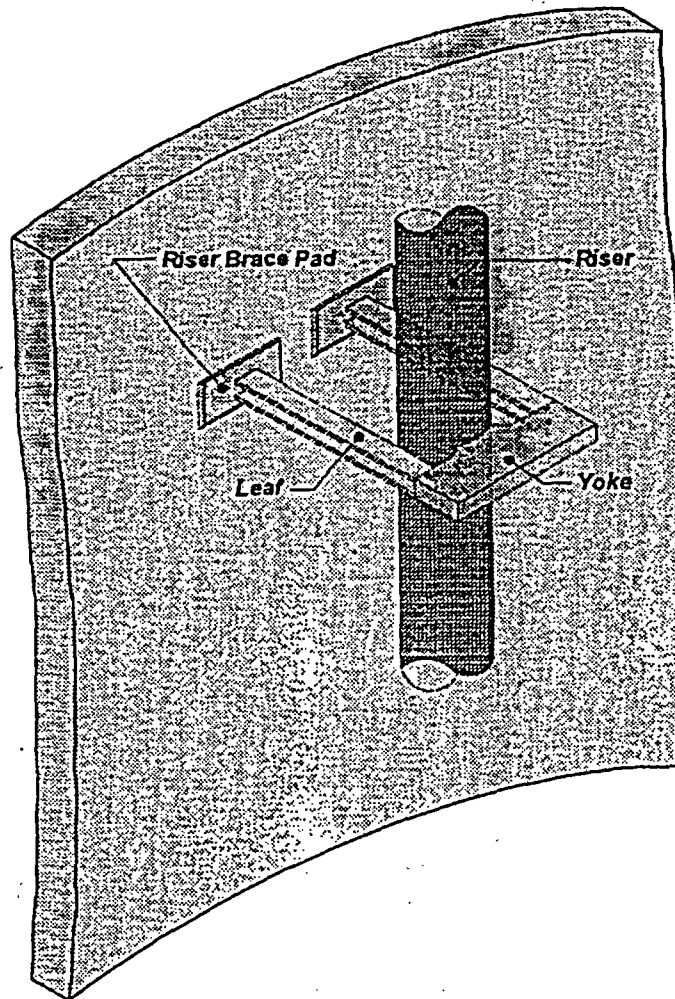


Figure 2.2. Hatch-1 Jet Pump Riser and Brace



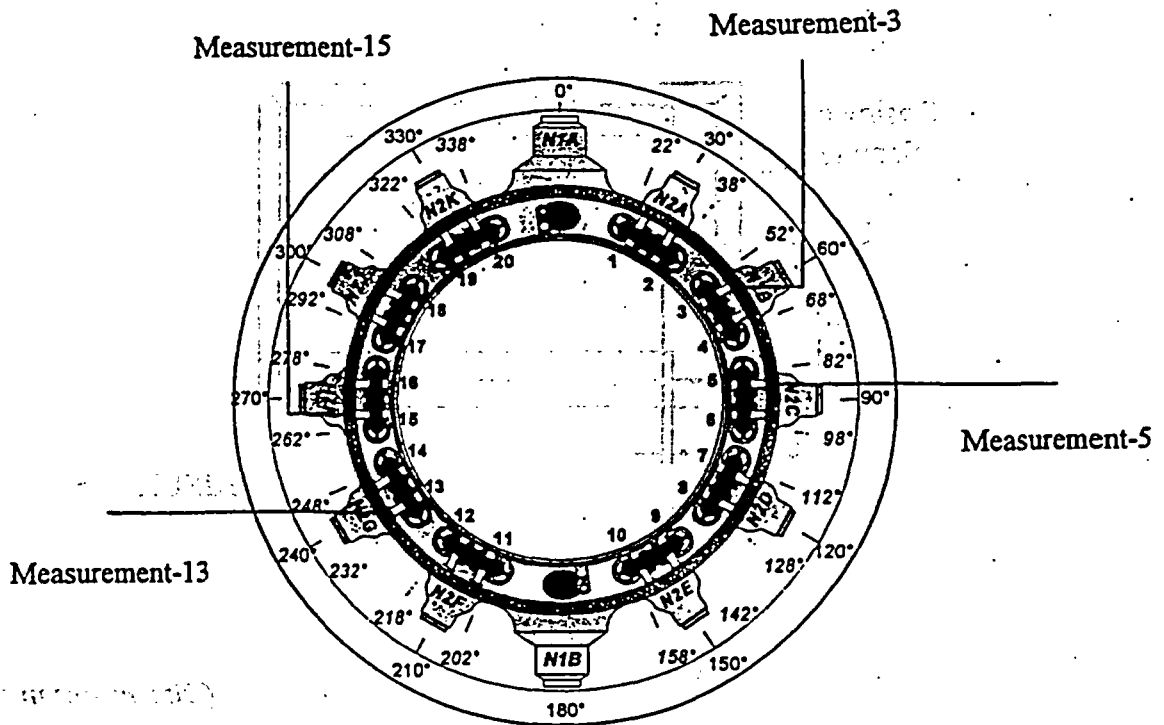
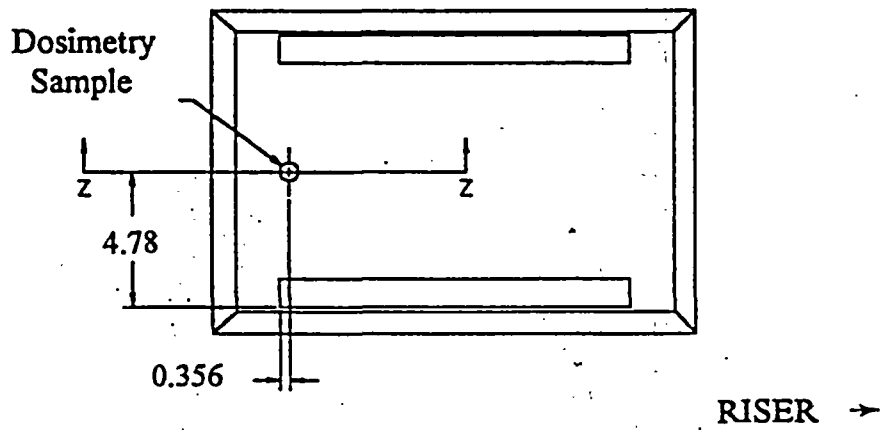


Figure 2.3. Azimuthal Locations of Hatch-1 Riser  
Brace Pad Dosimetry Measurements



*(Dimensions in cm)*

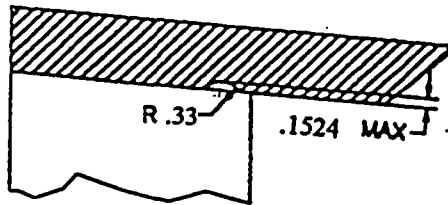


Figure 2.4. Location of Hatch-1 Brace Pad Dosimetry Samples Viewed from Inside the Vessel

## 3 HATCH-1 PLANT DATA

### 3.1 Introduction

Because of the strong attenuation of the neutron fluence between the core and the vessel (~ three to four decades depending on location) and the resulting sensitivity of the fluence transport calculation, an accurate and detailed description of the core/internals/vessel configuration is required. The data required for the calculation of the Hatch-1 riser brace pad measurements was requested from Southern Nuclear Operating Company in Reference-7. The data was provided in a series of transmittals including detailed drawings of the plant configuration and electronic files describing the core neutron source. Additional measurement related data was taken from Reference-3a and Reference-3b and core design data was taken from References 8-9. BNL reviewed this data and prepared the input required for the transport calculations. The data and input preparation were consistent with the requirements of Regulatory Guide 1.190.

### 3.2 Core, Internals and Vessel Geometry and Materials Data

The Hatch-1 core geometry and material composition data were taken from References 8-9 and the material provided by Southern Nuclear Operating Company. The core power level, inlet temperature and operating pressure are given in Table 3.2.1. Fuel assembly and core geometry configurations are given in Figures 3.2.1 and 3.2.2, respectively. Figure 3.2.1 illustrates a fuel assembly design with a 7x7 array of fuel pin cells. This design is representative of the early operating cycles of Hatch-1. Later cycles of Hatch-1 use 8x8 designs. Figure 3.2.1 illustrates that the Hatch-1 fuel assembly designs have non-uniform water gaps with alternate narrow and wide water gaps separating the neighboring fuel assemblies.

For this analysis, the fuel assembly material compositions were homogenized over the fuel assembly pitch, including the water gap. The brace pad measurements and vessel fluence are most sensitive to the fuel compositions of the assemblies in the outer-most rows of fuel assemblies. To account for the radial dependence of the core void distribution, region-specific average fuel assembly compositions were determined for the four regions defined in Figure 3.2.3: (1) inner core region, (2) outer core region (3) core boundary region and (4) the low void region. The axial void distributions were included. The use of the

group-average fuel compositions, rather than assembly-specific compositions, results in less than a ~1% error in the measurement predictions. Plant Process Computer (Reference 10) data was used to determine the coolant densities for Cycles 1-12 and core nodal calculations were used for Cycles 13-19. For convenience Cycles 1-4 were combined (Process Computer data for the 144 inch core), Cycles 5-12 were combined (Process Computer data for the 150 inch core) and Cycles 13-19 were combined (nodal calculation data with the 150 inch core). In combining this data, the cycle-specific data was weighted by the cycle exposure. The region-wise fuel compositions for Cycles 1-4, Cycles 5-12 and Cycles 13-19 are given in Tables 3.2.2 - 3.2.4, respectively, at the elevation of the dosimetry measurements.

The fuel number densities provided in Tables 3.2.2 - 3.2.4 for the  $^{235}\text{U}$ ,  $^{238}\text{U}$ , and  $\text{O}_{\text{fuel}}$  isotopes are appropriate for the DORT/TORT discrete ordinate methods, but not for RAMA. In addition to these isotopes, the RAMA method requires number densities for the  $^{239}\text{Pu}$ ,  $^{240}\text{Pu}$ ,  $^{241}\text{Pu}$ , and  $^{242}\text{Pu}$  isotopes. Furthermore, the ratio of U/Pu number densities must be consistent with fuel exposure. To generate the fuel material data needed for the RAMA fluence model, an 8x8 fuel assembly design typical of the later Hatch-1 core loadings was depleted. The uranium and plutonium number densities from the depletions were tabulated as functions of exposure and void fraction. Using the Hatch-1 fuel exposure and void data for each operating cycle, fuel number densities for the RAMA fluence model were determined. The coolant number densities in Tables 3.2.2 through 3.2.4 were used as provided.

The geometry and material data for the Hatch-1 vessel and internals were taken from drawings provided by Southern Nuclear Operating Company. The component dimensions for the core shroud, jet pump riser and mixer tubes, pressure vessel, mirror insulation, and biological shield are given in Table 3.2.1. The indicated geometry and materials apply at elevations in the neighborhood of the jet pump riser brace pads (viz., at axial elevations around 742.95 cm that is the mid-elevation of the jet pump brace assembly).

### 3.3 Jet Pump Riser Brace Pad Geometry and Materials Data

The local geometry surrounding the brace pad dosimetry locations is relatively complex due to the proximity of the jet pump mixer pipe, riser pipe, riser brace, core shroud and pressure vessel. The geometrical arrangement surrounding the brace pad dosimetry locations is given in Figures 2.2 - 2.4 and Figures 3.3.1 - 3.3.5. As indicated in Figures 2.2 and 2.4, the dosimetry samples were taken from the left-hand side of the left-hand brace pad (as viewed from the inside of the vessel). The dimensions of the brace pad and the relative location of the brace leaves on the pad are shown in Figure 3.3.2. As shown in Figure 3.3.3, the brace pads are located at an elevation of 742.95 cm (relative to the inside of the bottom of the vessel). As a reference, the core mid-plane is at an elevation of 712.622 cm. The dimensions of the riser brace are given in Figures 3.3.4 and 3.3.5.

The jet pump mixer pipe, riser pipe and brace are SS-304, and the brace pad is Inconel-182. The specific material compositions are given in Table 3.2.5.

### 3.4 Core Neutron Source Data

The core neutron source is determined by the three-dimensional power and exposure distributions. The power distribution is used to determine the spatial distribution of the fission rate and source density. The exposure distribution is used to account for the increased number and harder (more penetrating) spectrum of neutrons produced in plutonium fission.

The Southern Nuclear Operating Company provided the core power and fuel exposure distribution data for Cycles 1-19. The core neutron source was determined using the cycle-specific beginning-of-cycle (BOC) and end-of-cycle (EOC) three-dimensional burnup distributions. The three-dimensional exposure distributions for Cycles 1-12 were determined using Process Computer data based on plant Traversing In-core Probe (TIP) and Local Power Range Monitor (LPRM) neutron flux measurements. The source distributions for Cycles 13-19 were determined using calculated cycle-specific BOC and EOC three-dimensional burnup distributions.

Fuel bundle pin-wise power distributions were used to determine the radial source gradient for the three outermost rows of fuel bundles (i.e., the fuel bundles closest to the core boundary). The effect of the pin-wise source

gradient in the remaining inner fuel bundles is negligible (<1%) to the ex-core fluence problem and was not included in the analysis. The fuel bundle pin-wise power distribution data for Hatch-1 Cycles 1-19 was not available at the time of these calculations. However, since the source gradient effect has been determined to have an ~4% effect on the vessel fluence based on extensive earlier analyses, a set of typical pin powers was used in this analysis. The effect of this approximation is estimated to have a negligible effect (<1%) on the fluence predictions. The pin powers used in this analysis were taken from Reference-13.

Table 3.2.1 - Hatch-1 Core/Internals/Vessel Geometry and Materials Data

Reactor Parameter	Parameter Value	Material
Thermal Power	Cycles 1-16 - 2436 MW <sub>t</sub> Cycles 17-18 - 2558 MW <sub>t</sub> Cycle-19 - 2763 MW <sub>t</sub>	
Core Inlet Temperature	531°F	
Core Operating Pressure	1062 psia	
Core Saturated Temperature	551.7°F	
Inner Radius of Shroud	221.6150 cm	
Shroud Thickness	3.81 cm	SS-304
Inner Radius of RPV Liner	279.5588 cm	
Thickness of RPV Liner	0.7938 cm	SS-304
Inner Radius of RPV	280.3526 cm	
RPV Wall Thickness	13.6525 cm	A-533 B
Inner Radius - Insulation Liner*	307.880 cm	
Thickness of Insulation Liner*	0.159 cm	SS-304
Thickness of Insulation*	8.571 cm	A1
Inner Radius - Concrete Shield*	392.970 cm	
Thickness of Concrete Shield*	40.62 cm	Concrete
Center-Line Radius of the Riser	246.8118 cm	
Number of Jet Pumps	20	
Location of Jet Pumps	± 8.1771° of Riser	
Location of Risers	At 30° intervals starting at 30°**	
Jet Pump Inside Diameter	16.4592 cm	SS-304
Jet Pump Outside Diameter	18.9992 cm	
Riser Inside Diameter	25.7454 cm	SS-304
Riser Outside Diameter	27.3050 cm	

\* The material, thickness and separation from the pressure vessel of the insulation and concrete shield have been taken to be the same as the BWR benchmark problem of NUREG-6115.

\*\* The core flats are 0°, 90°, 180° and 270°. There are no risers at the two recirculation suction nozzles at 0° and 180°.

Table 3.2.2 Cycle 1-4 Core Material Compositions

Material	Component	Densities (atoms/barn-cm)
Inner Core	H	2.0627-02
	O	1.0313-02
	O (Fuel)	1.0677-02
	U-235	5.4093-05
	U-238	5.2025-03
	Zr	5.7167-03
Outer Core	H	2.1678-02
	O	1.0839-02
	O (Fuel)	1.0677-02
	U-235	5.4093-05
	U-238	5.2025-03
	Zr	5.7167-03
Core Boundary	H	2.1586-02
	O	1.0793-02
	O (Fuel)	1.0677-02
	U-235	5.4093-05
	U-238	5.2025-03
	Zr	5.7167-03
Low Void Region	H	2.4165-02
	O	1.2082-02
	O (Fuel)	1.0677-02
	U-235	5.4093-05
	U-238	5.2025-03
	Zr	5.7167-03

Table 3.2.3 Cycle 5-12 Core Material Compositions

Material	Component	Densities (atoms/barn-cm)
Inner Core	H	2.0021-02
	O	1.0011-02
	O (Fuel)	1.0677-02
	U-235	5.4093-05
	U-238	5.2025-03
	Zr	5.7167-03
Outer Core	H	2.1448-02
	O	1.0724-02
	O (Fuel)	1.0677-02
	U-235	5.4093-05
	U-238	5.2025-03
	Zr	5.7167-03
Core Boundary	H	2.2210-02
	O	1.1105-02
	O (Fuel)	1.0677-02
	U-235	5.4093-05
	U-238	5.2025-03
	Zr	5.7167-03
Low Void Region	H	2.4480-02
	O	1.2240-02
	O (Fuel)	1.0677-02
	U-235	5.4093-05
	U-238	5.2025-03
	Zr	5.7167-03

Table 3.2.4 Cycle 13-19 Core Material Compositions

Material	Component	Densities (atoms/barn-cm)
Inner Core	H	1.7898-02
	O	8.9489-03
	O (Fuel)	1.0677-02
	U-235	5.4093-05
	U-238	5.2025-03
	Zr	5.7167-03
Outer Core	H	2.0461-02
	O	1.0231-02
	O (Fuel)	1.0677-02
	U-235	5.4093-05
	U-238	5.2025-03
	Zr	5.7167-03
Core Boundary	H	2.3173-02
	O	1.1587-02
	O (Fuel)	1.0677-02
	U-235	5.4093-05
	U-238	5.2025-03
	Zr	5.7167-03
Low Void Region	H	2.5168-02
	O	1.2584-02
	O (Fuel)	1.0677-02
	U-235	5.4093-05
	U-238	5.2025-03
	Zr	5.7167-03



Table 3.2.5 Vessel and Internals Material Compositions

Material	Component	Densities (atoms/barn-cm)
SS-304	Cr	1.74000E-02
	Mn	1.52000E-03
	Ni	8.55000E-03
	Fe	5.83000E-02
	C	2.37000E-04
	Si	8.93000E-04
A-533 B	Fe	8.265800E-02
	Ni	4.418000E-04
	Mn	1.115800E-03
	C	9.814000E-04
Insulation	Al	6.060300E-03
Brace Pad/Inconel-182	Cr	1.4365E-02
	Mn	6.5263E-03
	Fe	6.5280E-03
	Ni	6.0129E-02
	Nb	8.5000E-04
Concrete	H	1.51367E-02
	C	2.24032E-04
	O	8.53268E-02
	Na	2.04551E-03
	Mg	2.88319E-04
	Al	4.65596E-03
	Si	3.07780E-02
	K	1.35003E-03
	Ca	4.46115E-03
Fe	6.09755E-04	

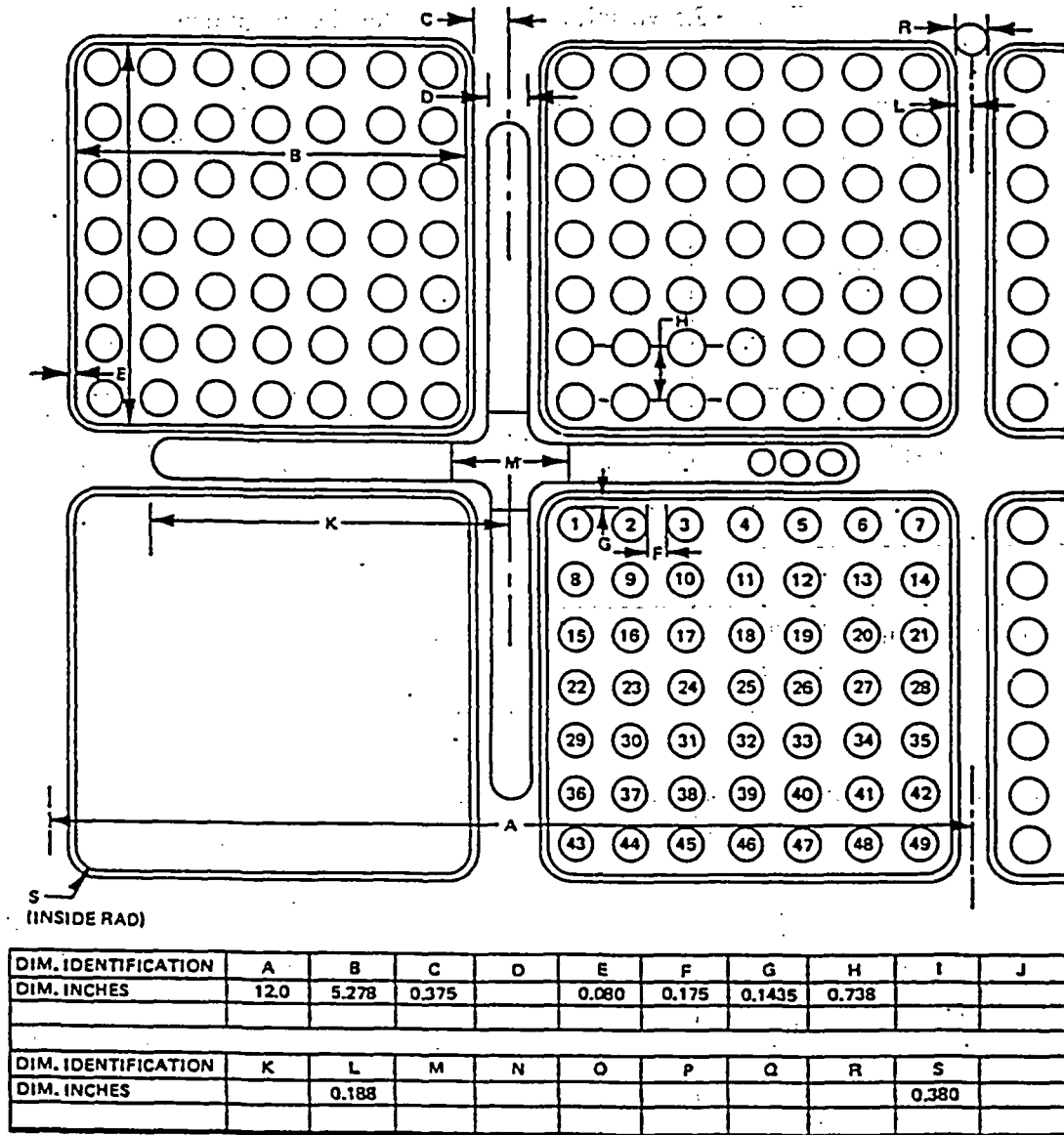


Figure 3.2.1. Hatch-1 Fuel Assembly Lattice Geometry

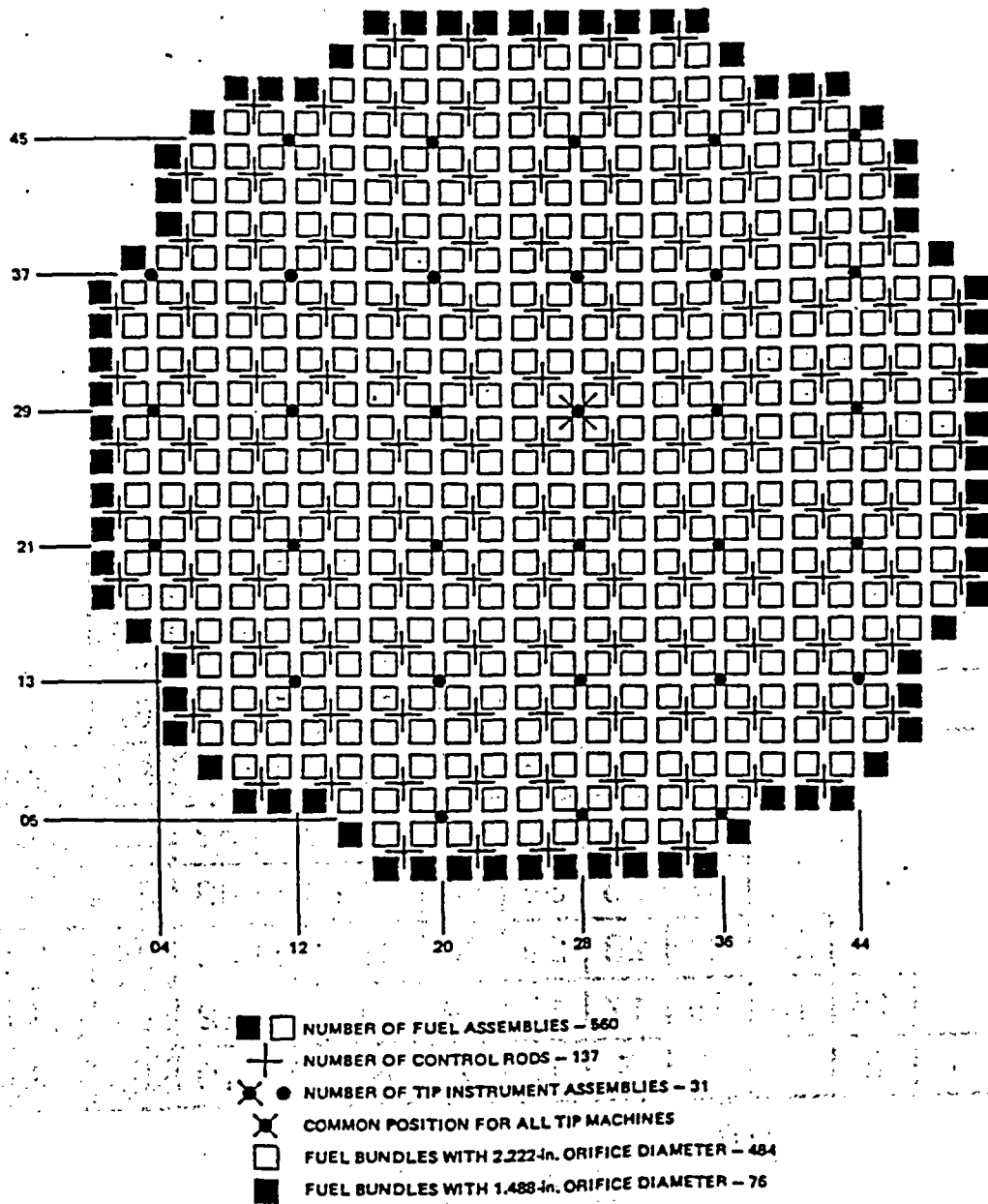


Figure 3.2.2. Hatch-1 Core Configuration

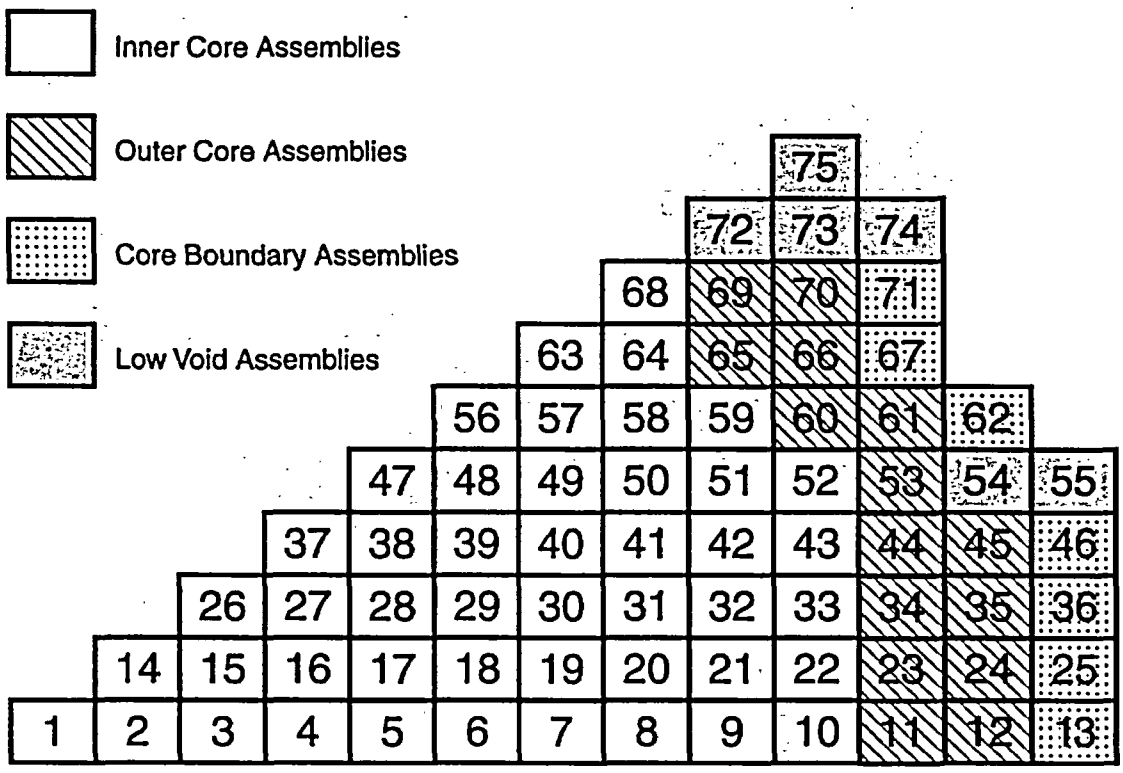


Figure 3.2.3. Radial Fuel Assembly Material Groups

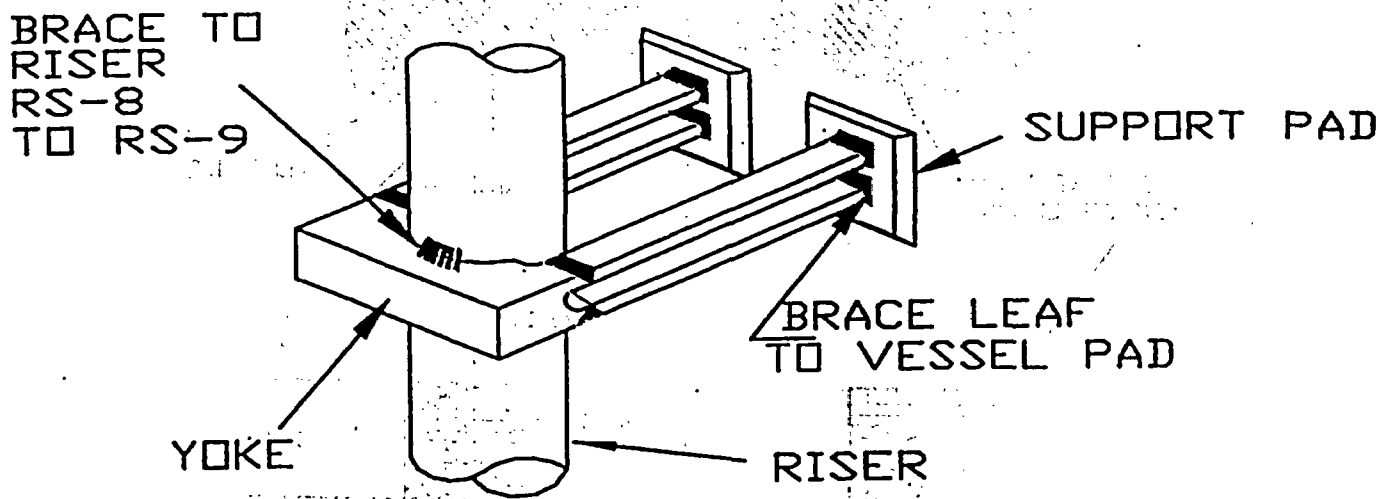


Figure 3.3.1. Hatch-1 Jet Pump Riser and Brace Configuration

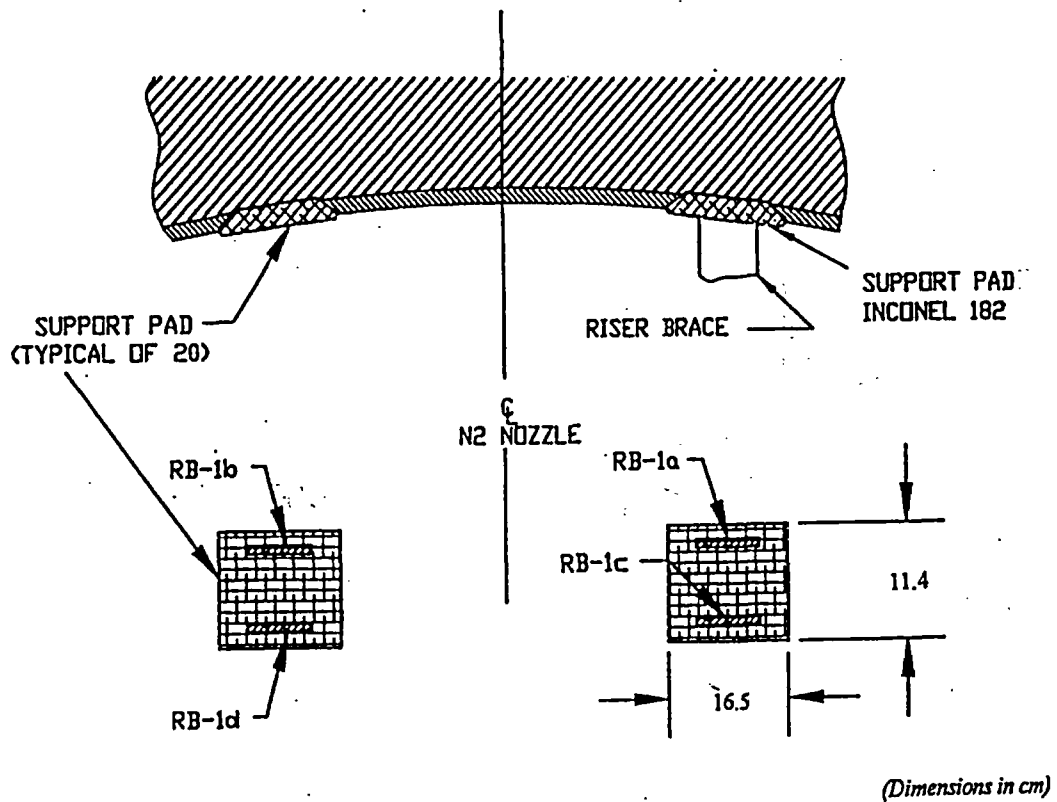


Figure 3.3.2. Azimuthal Location of Jet Pump Riser Brace Pad on Pressure Vessel

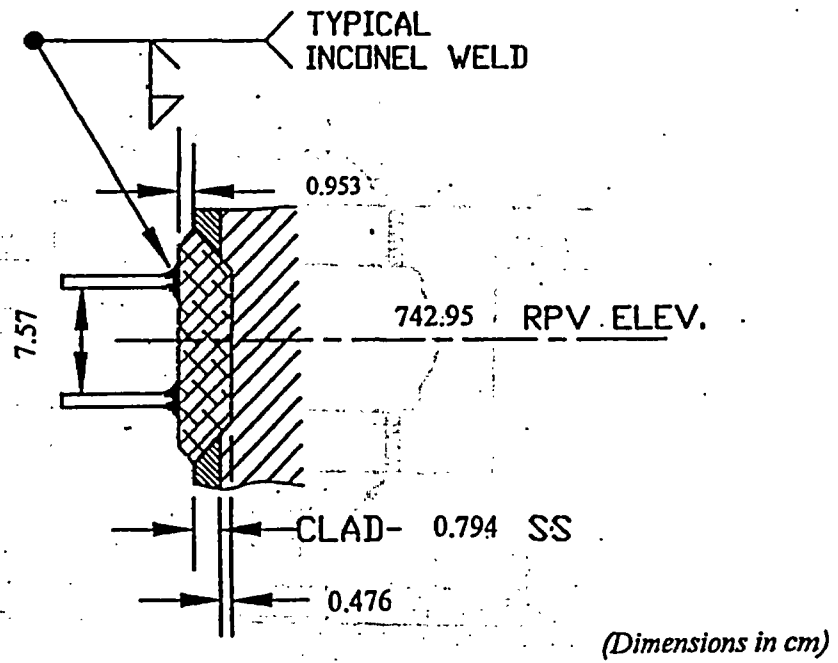


Figure 3.3.3. Horizontal View of Jet Pump Riser Brace Pad

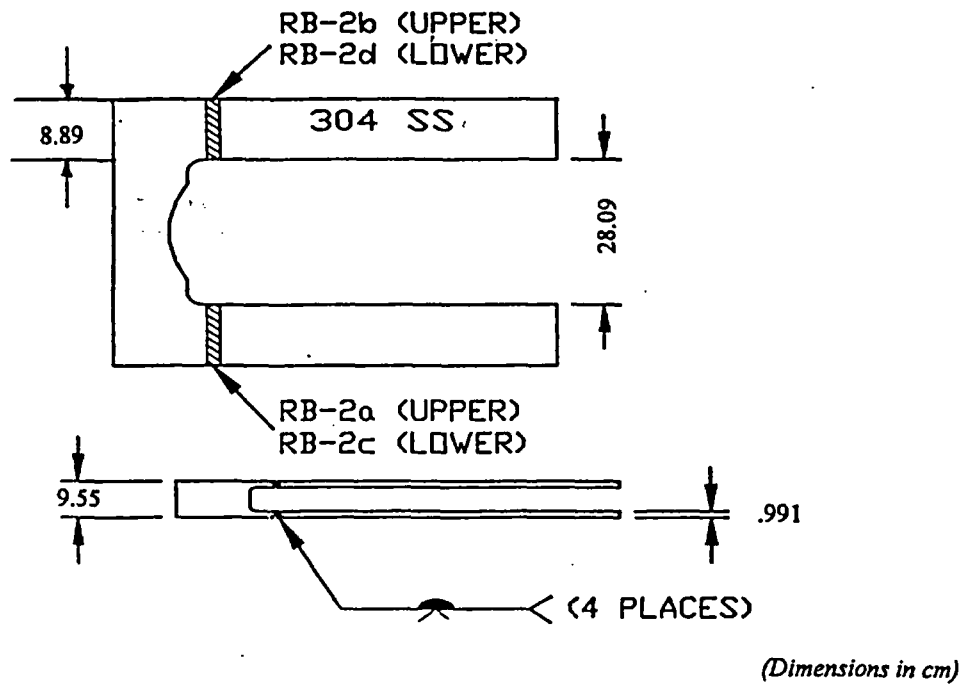
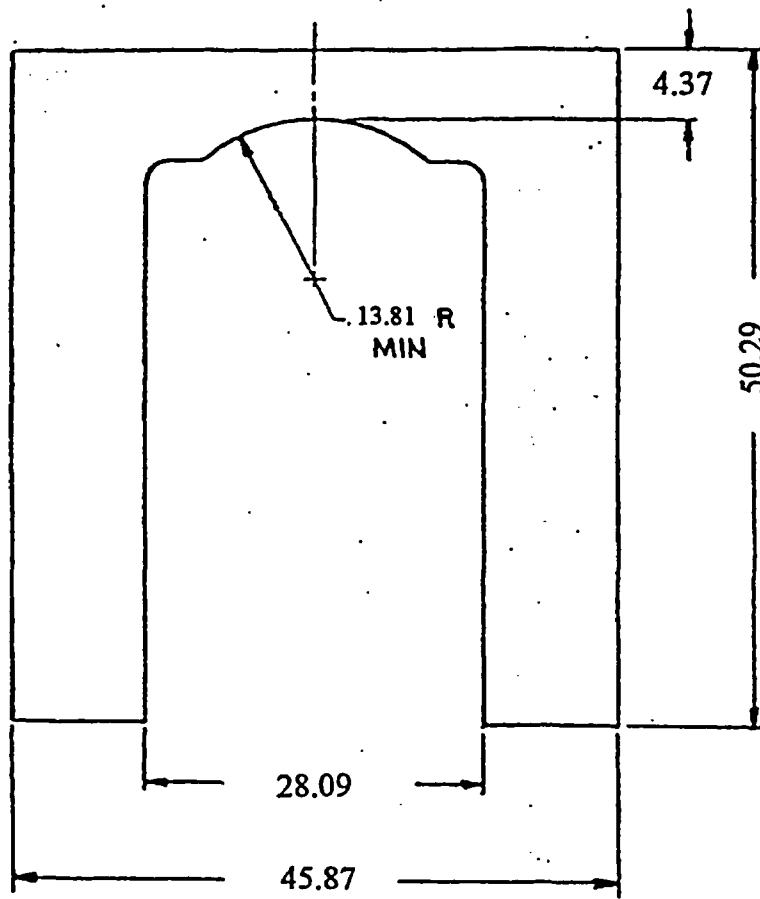


Figure 3.3.4. Horizontal and Vertical View of Jet Pump Riser Brace





*(Dimensions in cm)*

Figure 3.3.5. Vertical View of Jet Pump Riser Brace

## 4 CALCULATIONAL METHODS

### 4.1 Introduction

The DORT/TORT (used at BNL) and RAMA (used at TWE) methodologies used to perform the Hatch-1 jet pump riser brace pad measurements generally follow the methods and approach described in Regulatory Guide 1.190 for pressure vessel fluence calculation and measurement methods. However, the present calculations have a somewhat broader application in that Regulatory Guide 1.190 is primarily concerned with the fast fluence while the present analysis also requires the determination of the thermal neutron fluence. In addition, the calculation of the brace pad measurements requires the modeling of the relatively complex three-dimensional riser/brace/vessel geometry surrounding the brace pad sample locations (see Figures 2.2 and 3.3.1), which is typically not required in the determination of the vessel fluence.

The nuclear cross sections, determination of the core neutron source, transport calculations, DORT/TORT synthesis approach, and the dosimetry cross sections are described in the Sections 4.2-4.2.1, 4.3-4.3.1, 4.4-4.4.3, respectively. The method used to determine the thermal neutron fluence is described in Section 4.4.4 and the methods used to model the local riser/brace/vessel geometry are described in Section 4.4.5

The RAMA fission spectra and the RAMA source are described in sections 4.2.2 and 4.3.2 respectively. The neutron transport calculations, fluence model, dosimetry cross-sections, and thermal fluence calculation are described in sections 4.5-4.5.4, respectively.

### 4.2 Neutron Cross Sections and Fission Spectra

The DORT/TORT and RAMA neutron transport calculations were performed using data from the BUGLE-96 data library (Reference-11). The BUGLE-96 library provides a 47 neutron/20 gamma-ray broad-group energy representation for determining neutron and photon space-energy distributions in light water reactor shielding and pressure vessel fluence applications. The BUGLE-96 library was determined by collapsing the ENDF/B-VI VITAMIN-B6 fine-group cross section set using spatially dependent spectra typical of light water reactor configurations. Special tabulations of cross-sections are provided in BUGLE-96 for core materials typical of a BWR operating

environment. The BUGLE-96 library includes the ENDF/B-VI updates of the iron, hydrogen and oxygen cross sections, which are known to have a significant effect on pressure vessel fluence predictions.

#### 4.2.1 DORT/TORT Fission Spectra

The fission spectra for U-235, U-238, and Pu-239 that were used for the DORT/TORT transport calculations were taken from BUGLE-96. The fission spectrum for Pu-241 was determined with NJOY using ENDF/B-VI data. These spectra were used in the MESH (Reference-12) calculations that prepare the core neutron source for the DORT/TORT calculations.

#### 4.2.2 RAMA Fission Spectra

The fission spectra for U-235, U-238, Pu-239, Pu-240, Pu-241, and Pu-242 that are used in the RAMA transport calculations were taken directly from the latest release of the BUGLE-96 data library. RAMA calculates a weighted fission spectrum based on the relative contributions of the fuel isotopes that is used in the transport calculation.

### 4.3 Core Neutron Source

The Hatch-1 core neutron source for both the DORT/TORT and RAMA transport calculations was determined using the cycle-specific BOC and EOC three-dimensional burnup distributions. The source distributions accounted for the radial power gradient in the fuel assemblies loaded near the core boundary by modeling the pin-wise source distributions in the outer three rows of fuel assemblies. The magnitude of the neutron source accounts for the contribution of plutonium fissions as a function of fuel assembly exposure.

#### 4.3.1 DORT/TORT Source Calculation

The DORT/TORT source distribution was specified cycle-wise for each assembly and for each fifteen cm axial node. The MESH code was used to allocate the pin-wise power to the individual DORT ( $r$ ,  $\theta$ ) mesh blocks. This allocation was performed by a numerical integration of the power distribution, defined on the

(x, y) pin-wise mesh, over the (r,  $\theta$ ) mesh block. This numerical integration typically employed  $\geq 100$  integration mesh points per fuel pin and was shown to be accurate to within  $\leq 1\%$  for each (r,  $\theta$ ) mesh block.

The magnitude of the neutron source increases with fuel burnup due to the higher number of neutrons released per MeV of energy produced by Pu fission. This was taken into account by calculating the number of neutrons per MeV,  $\nu/\kappa$  [neutrons/MeV], using the fuel burnup dependent isotopic fission fractions provided by Southern Nuclear Operating Company and given in Table 4.2.1. In addition, the fission spectrum was considered to be dependent on the fuel burnup in order to account for the harder more penetrating neutron spectrum characteristic of the Pu fissions in the high burnup fuel. This exposure dependence was also determined using the Table 4.2.1 data and was included in the DORT source distribution.

### 4.3.2 RAMA Source Calculation

The neutron source for the RAMA transport calculation is calculated in RAMA using the input power density factors for the different fuel regions and data from the RAMA nuclear data library. The fission spectrum used in the RAMA source calculation is described in Section 4.2.2. The RAMA nuclear data library provides the cross section data (including fission cross sections), neutron release factors ( $\nu$ ), and energy release factors ( $\kappa$ ) needed to convert the input powers to source terms.

The RAMA core model is constructed to replicate the nodal geometry used in core simulator codes and process computers, including appropriate representations for the pin-wise power and source term distributions in the outer rows of fuel assemblies. In the current analysis, BNL provided three-dimensional relative power distributions for the core region and pin-wise power distributions for the fuel assemblies for each Hatch-1 operating cycle. Appropriate uranium and plutonium number densities for the fission spectrum calculation were not available for RAMA, therefore fuel assembly depletion calculations were performed using a fuel assembly design typical of the later Hatch-1 operating cycles. Using the cycle-dependent exposure data provided for Hatch-1, uranium and plutonium number densities for each fuel region were calculated from the fuel assembly depletion data and used in the source calculation.

## 4.4 DORT/TORT Neutron Transport Calculations (BNL)

### 4.4.1 Neutron Transport Method

The DORT/TORT transport calculations were performed in a fixed source mode for a radial (r,  $\theta$ ) plane, an axial (r, z) plane, and in a one-dimensional (r) geometry. The calculational model represented a one-eighth azimuthal sector of the core and vessel geometry. The Hatch-1 planar and axial geometries used in the DORT analysis are given in Figures 4.1 and 4.2, respectively.

The transport calculations were performed using an  $S_8$  quadrature and a P-3 angular decomposition of the scattering cross-sections. The (r,  $\theta$ ) mesh included 72 angular mesh intervals, and 226 radial mesh intervals. The angular ( $\theta$ ) and radial (r) mesh densities were increased at material interfaces where the geometry was changing rapidly and at the measurement locations. The radial mesh used in the axial (r, z) calculations was essentially identical to that used in the (r,  $\theta$ ) calculations. The axial model included 179 mesh intervals for Cycles 1-4 where the fuel length was 144 inch and 183 mesh intervals for Cycles 5-19 where 150 inch fuel was used.

Vacuum boundary conditions were used on the outer radial and axial boundaries of the problems and reflecting boundary conditions were used on the internal  $\theta = 0^\circ$  and  $\theta = 45^\circ$  azimuthal boundaries. A pointwise flux convergence of  $10^{-3}$  was used together with an integrated flux convergence criteria of  $10^{-3}$ .

### 4.4.2 Flux Synthesis Method

The vessel fluxes were determined using the flux synthesis method of NUREG/CR-6115, BNL-NUREG-52395 (Reference-13) to combine the DORT (r,  $\theta$ ) and DORT (r, z) calculated fluxes. The flux at the (r,  $\theta$ , z) location was determined by the relation

$$\phi_g(r, \theta, z) = [\phi_g(r, \theta)/\phi_g(r)]\phi_g(r, z), \quad (1)$$

where  $\phi_g(r, \theta)$ ,  $\phi_g(r, z)$  and  $\phi_g(r)$  are the group-g fluxes calculated in the indicated geometry. The effective core radius  $R_{eff}$  used in the cylindrical geometry (r, z) and (r) calculations was determined so that the flux above 1-MeV,  $\phi_{>1}$ , at the vessel inner-wall satisfies

the condition

$$\phi_{>1}(r; R_{eff}) = \frac{1}{2\pi} \int_0^{2\pi} \phi_{>1}(r, \theta) d\theta. \quad (2)$$

The radial source distribution in these cylindrical calculations was determined as an azimuthal average of the  $(r, \theta)$  source distribution.

#### 4.4.3 Dosimetry Cross Sections

The reaction rates for the riser brace pad samples were determined by counting and analysis at PNNL (Reference-3a and Reference-3b). BNL calculated a 47 group spectrum for the Hatch-1 plant at the radial location of the brace pad using DORT and the BUGLE-96 library. Fast reaction rates were determined for the dosimeter measurements listed in Table 2.1 using ENDF/B-VI cross section data and the BNL supplied Hatch-1 spectrum. PNNL calculated the fast ( $>0.1$  MeV and  $>1.0$  MeV) cross sections (Reference-3b) based on the ENDF/B-VI dosimetry file collapsed in 100 groups using the BNL Hatch-1 spectrum. The cross sections for the thermal dosimetry reactions of Table 2.1 were calculated at BNL by averaging the MATXS-12 library (Reference-14) reaction cross sections over the thermal portion of the BNL Hatch-1 69 group neutron spectrum at the location of the brace pad samples.

#### 4.4.4 Thermal Fluence Calculation

The ratio of the thermal fluence to the fast  $>1$  MeV fluence at the measurement location was determined using a detailed one-dimensional model of the downcomer/brace-pad interface. The calculations were performed with BUGLE-96 cross sections and included up-scattering in the thermal groups. The neutron spectrum was edited at the brace-pad depth of the measured dosimetry samples, and the ratio of the  $E < 0.414$  eV thermal fluence to the  $E > 1$  MeV fast fluence was determined. This ratio was used as an ad-hoc multiplier, applied to the TORT calculated fast fluence, to determine the thermal fluence to be compared with measurement.

#### 4.4.5 TORT Calculations of the Effect of the Local Brace Pad Geometry

The geometrical arrangement of the riser, brace and vessel introduces a three-dimensional spatial dependence into the transport calculation of the brace pad measurements. In order to evaluate the effect of the local geometry on the measurements, three-dimensional TORT calculations were performed with and without the jet pump brace present. The TORT model represented an  $(r, \theta, z)$  segment of the geometry including: (1) the radial geometry from the inside of the shroud to the outside of the vessel (2) an azimuthal section from  $0^\circ$  (at the core flats) to  $8.2^\circ$  (passing through the center of the neighboring jet pump) and (3) a 30.5 cm axial section centered on the jet pump brace.

The TORT calculation was performed using an  $(x, y, z)$  model in which the cylindrical riser and jet pump cross-sectional areas were preserved. The shroud and vessel were considered to be flat, since the amount of curvature introduced over this small section ( $\leq 1$  cm radial deviation from linearity over the entire brace pad) has a negligible effect on the calculated fluence ratios. The TORT geometry is shown in Figures 4.3-4.5. Source boundary conditions, determined using a full three-dimensional DORT synthesis model, were specified on all six external surfaces.

The results of the TORT calculations by BNL with and without the riser brace and brace pads included are presented in Table 4.2.2. The calculated adjustment factor (B/A) is the ratio of: (1) the calculated fluence at the location of the samples on the riser brace pad with the full riser brace and pad geometry included and (2) the calculated sample fluence without the riser brace and pad present.

To account for the local three-dimensional geometry effects of the riser brace/pad geometry on the DORT measurement calculations, the B/A ratio of the TORT predictions with and without the riser brace and pads present was applied as a multiplicative adjustment to the DORT calculations.

## 4.5 RAMA Neutron Transport Calculations (TWE)

### 4.5.1 Neutron Transport Method

The RAMA Fluence Methodology (TWE) supports a full three-dimensional transport solver that provides direct solutions of the neutron flux, fluence, and activation. The RAMA geometry modeling capability is based upon combinatorial geometry techniques. This allows models to be built with accurate representations of component shapes, dimensions, and position in the reactor, including the mixing of rectangular and cylindrical body surfaces.

The transport calculation is based upon a three-dimensional deterministic volume integral technique with treatments for fixed-source and anisotropy. The user may select the angular quadrature for the transport calculation. An  $S_8$  quadrature was used for this analysis. Anisotropy is treated with high order angular decompositions of the scattering cross-sections. In this analysis, the heavy nuclides are treated with a P-5 and lighter nuclides with a P-7 Legendre expansion of the scattering cross-sections. A pointwise flux convergence criterion of  $10^{-2}$  was used in the transport calculation.

The RAMA transport methodology includes integrated capabilities for calculating the fission spectrum and neutron source for the transport calculation from common user input parameters and information provided in the nuclear data library.

The RAMA methodology calculates fluence and activation using the neutron flux distributions calculated by the transport calculation, isotopic activation and decay chains, and reactor daily operating history.

The RAMA methodology includes a nuclear data library that contains cross-section data and nuclear constants for several reactor material nuclides. The RAMA cross-section data is derived from the BUGLE-96 data library and are represented in the same 47-neutron/20-gamma energy groups. The RAMA data library includes additional cross-section data for the  $^{239}\text{Pu}$ ,  $^{240}\text{Pu}$ ,  $^{241}\text{Pu}$ , and  $^{242}\text{Pu}$  fuel isotopes and other nuclear data constants including energy release per fission ( $\kappa$ ) factors that are needed for the RAMA source and transport calculations.

### 4.5.2 The RAMA Fluence Model

The RAMA fluence model for Hatch-1 is illustrated in Figure 4.6. The RAMA model assumes octant symmetry in which the north-northeast octant is represented in the azimuthal dimension. Assuming mirror reflection along the diagonal boundary, the RAMA model solves the same problem as the east-northeast DORT/TORT model illustrated in Figure 4.1 (not to scale).

Vacuum boundary conditions are used on the outer radial and axial boundary surfaces of the problem. Reflective boundary conditions are used on the internal surfaces for the 0 and 45 degree azimuths. Figure 4.6 shows the basic reactor geometry near the axial elevation corresponding to the jet pump brace assembly. The RAMA model uses square rectangular bodies to represent the fuel assembly geometries and cylindrical bodies to describe the ex-core regions and components.

Appropriate combinations of bodies are used in the core reflector region between the core region and shroud to describe the transition from planar to cylindrical geometries. Figure 4.6 also shows that the jet pump riser pipe, mixer pipes, and yoke assembly are appropriately represented in the downcomer region of the model. Assuming symmetry conditions, each of the jet pumps 3, 5, 13, and 15 are appropriately accounted for in the RAMA model.

Figure 4.2 (not to scale) provides an axial representation of the Hatch-1 reactor, including noting the axial elevations around the jet pump brace assembly. The RAMA model used the same axial elevation information. The RAMA model agreed with that shown in Figure 4.2 with the following exceptions: (1) the jet pump assemblies were explicitly modeled in the downcomer region between radial dimensions 225.425 and 279.559 cm and (2) the axial extent of the RAMA model spanned the elevations 651.6624 to 834.5424 cm, relative to reactor vessel zero. It was determined by parametric study that this axial elevation range modeled in the RAMA transport code produced an asymptotic solution at the brace pad elevation of 742.95 cm (shown in Figure 3.3.3):

Figures 4.7 and 4.8 illustrate the detail of the Hatch-1 brace pad model used in the RAMA calculations. Figure 4.7 provides an axial view (side view) of the jet pump riser brace assembly. The brace assembly was modeled in the correct geometrical form with the following exceptions: (1) the upper leaf was homogenized with the water above the leaf to the top of the brace

pad to avoid small axial heights in the flux model; (2) the lower leaf was homogenized with the water below the leaf to the bottom of the brace pad to avoid small axial heights in the flux model; and (3) the yoke was expanded axially to coincide with the axial extent of the brace assembly after the adjustments in (1) and (2). Note that the brace pad is recessed into the reactor pressure vessel (RPV) cladding to interface with the RPV wall. Figure 4.8 provides a front view (looking out from the core region) of the jet pump riser brace pad. This figure shows that the full dimensional size of the brace pad is modeled and the radial and axial location where the sample was extracted.

The three-dimensional production model for the RAMA analysis contains 30,108 mesh regions. This model was used in the RAMA transport calculations for each of the 19 cycles of operating history data.

### 4.5.3 Dosimetry Cross Sections

The RAMA reaction rates for the fast activation reactions were determined by TWE for the dosimeter measurements given in Table 2.1 using the flat spectrum weighted response functions provided in the RAMA nuclear data library. The RAMA response functions were derived from the BUGLE-96 data library. The thermal reaction cross sections were determined by collapsing the 199 group VITAMIN-B6 (Reference-15) reaction cross sections to the 47 group BUGLE-96 structure using a BWR downcomer spectrum.

### 4.5.4 Thermal Fluence Calculation

The thermal fluence at the measurement location was determined using a detailed model of the downcomer, jet pump assembly, brace assembly, and brace pad interface. The thermal calculations included up-scattering in the thermal groups. The thermal fluence was edited for energy  $< 0.414$  eV at the brace pad depth of 0.1524 cm of the measured dosimetry samples. The thermal fluence calculated directly by the RAMA Fluence Methodology was compared with the measurements.

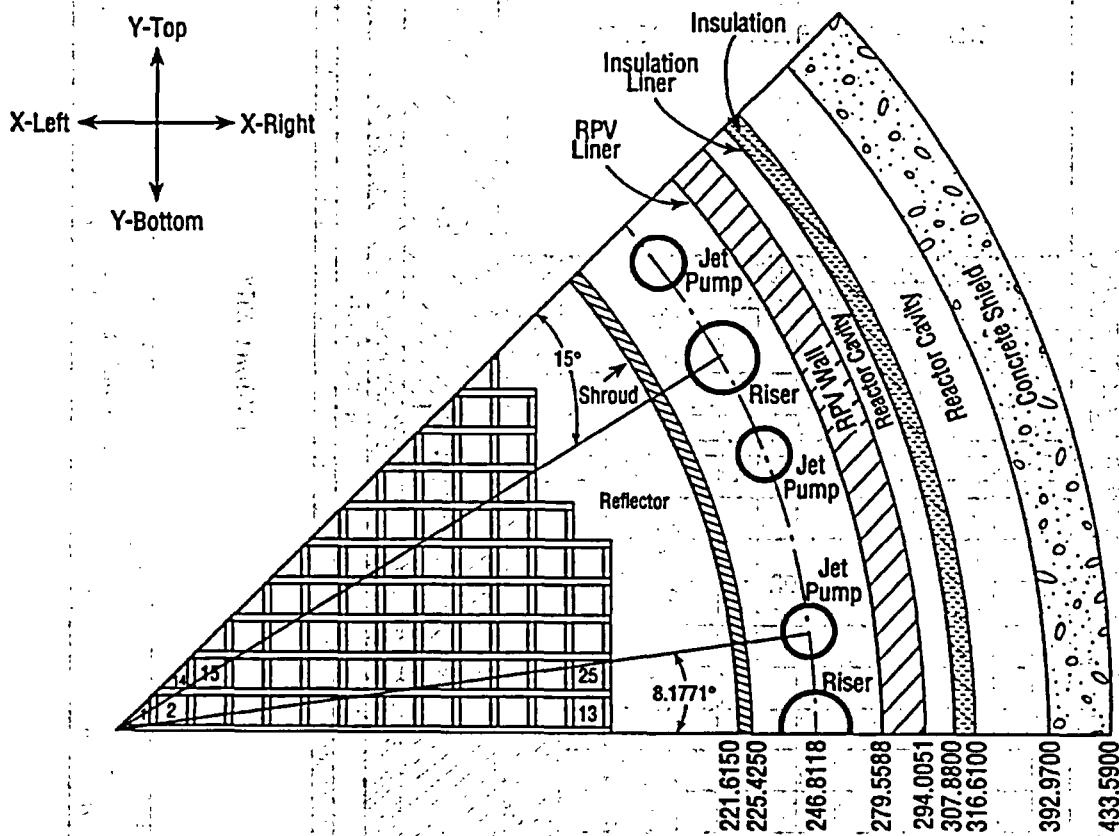
Table 4.2.1 - Fraction of Fissions by Isotope as a Function of Fuel Exposure.

Fuel Exposure (GWD/t)	U-235	U-238	Pu-239	Pu-241
0.0	0.9247	0.0753	0.0000	0.0000
5.0	0.6823	0.0770	0.2243	0.0164
10.0	0.5460	0.0818	0.3381	0.0341
15.0	0.4432	0.0836	0.4143	0.0589
20.0	0.3590	0.0886	0.4637	0.0887
25.0	0.2843	0.0887	0.5056	0.1214
30.0	0.2169	0.0924	0.5398	0.1510
35.0	0.1472	0.0942	0.5663	0.1923

Table 4.2.2 - TORT Calculations of the Effect of the Riser Brace and Brace Pad on the Dosimetry Measurements.

RESPONSE	A - Response at Sample Location w/o Riser Brace and Pad	B - Response at Sample Location with Riser Brace and Pad	Effect of Brace and Pad on Response B / A - Adjustment
> 1.0 MeV (n/cm <sup>2</sup> -sec)	1.1323 +9	1.1660 +9	1.0298
> 0.1 MeV (n/cm <sup>2</sup> -sec)	2.0857 +9	2.2155 +9	1.0622

# Hatch-1 Planar Geometry



NOTE: All Dimensions in cm

Figure 4.1. Hatch-1 Planar Geometry



## Hatch-1 Axial Geometry (Core flats at $\theta = 0^\circ$ )

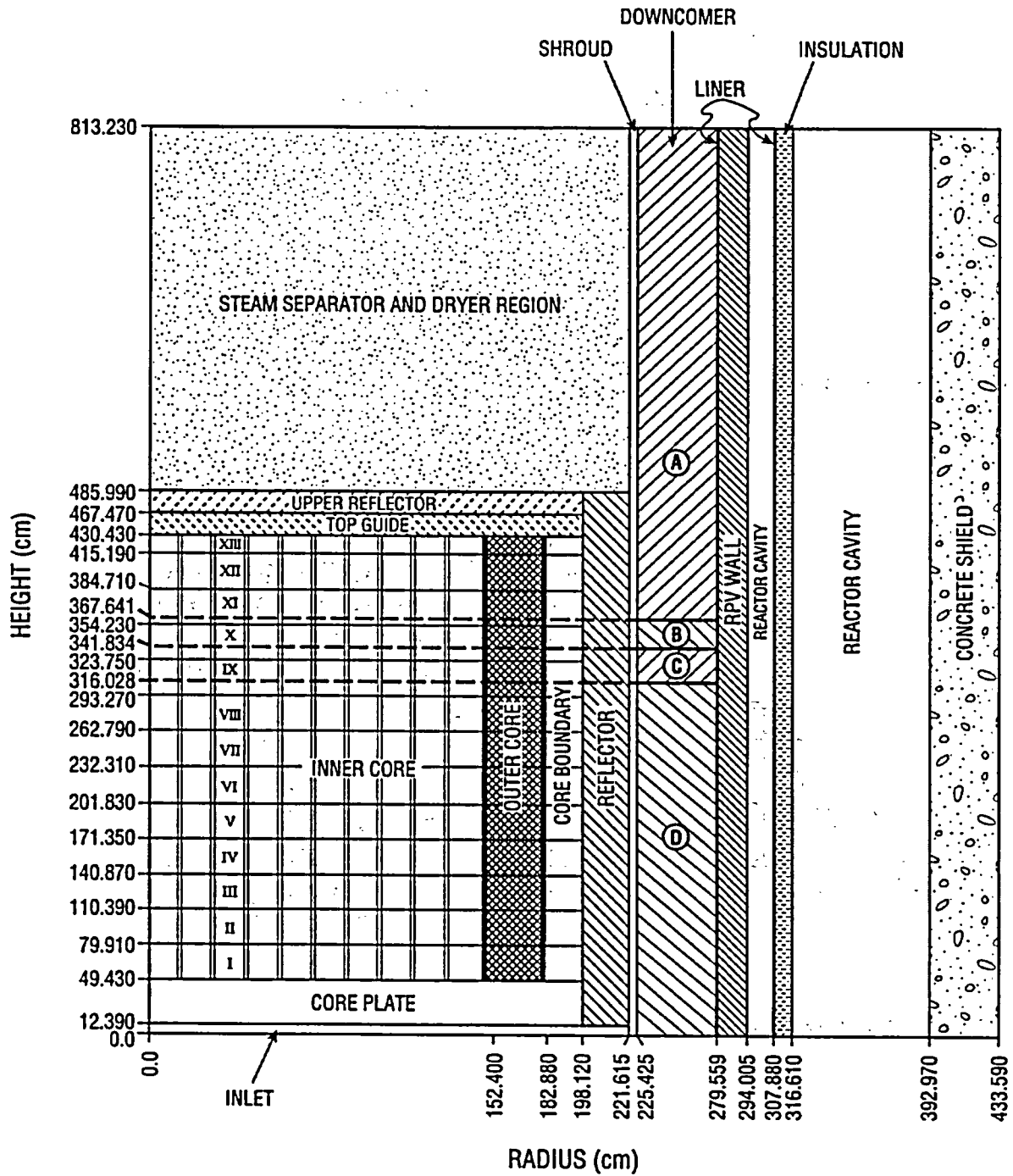


Figure 4.2. Hatch-1 Axial Geometry

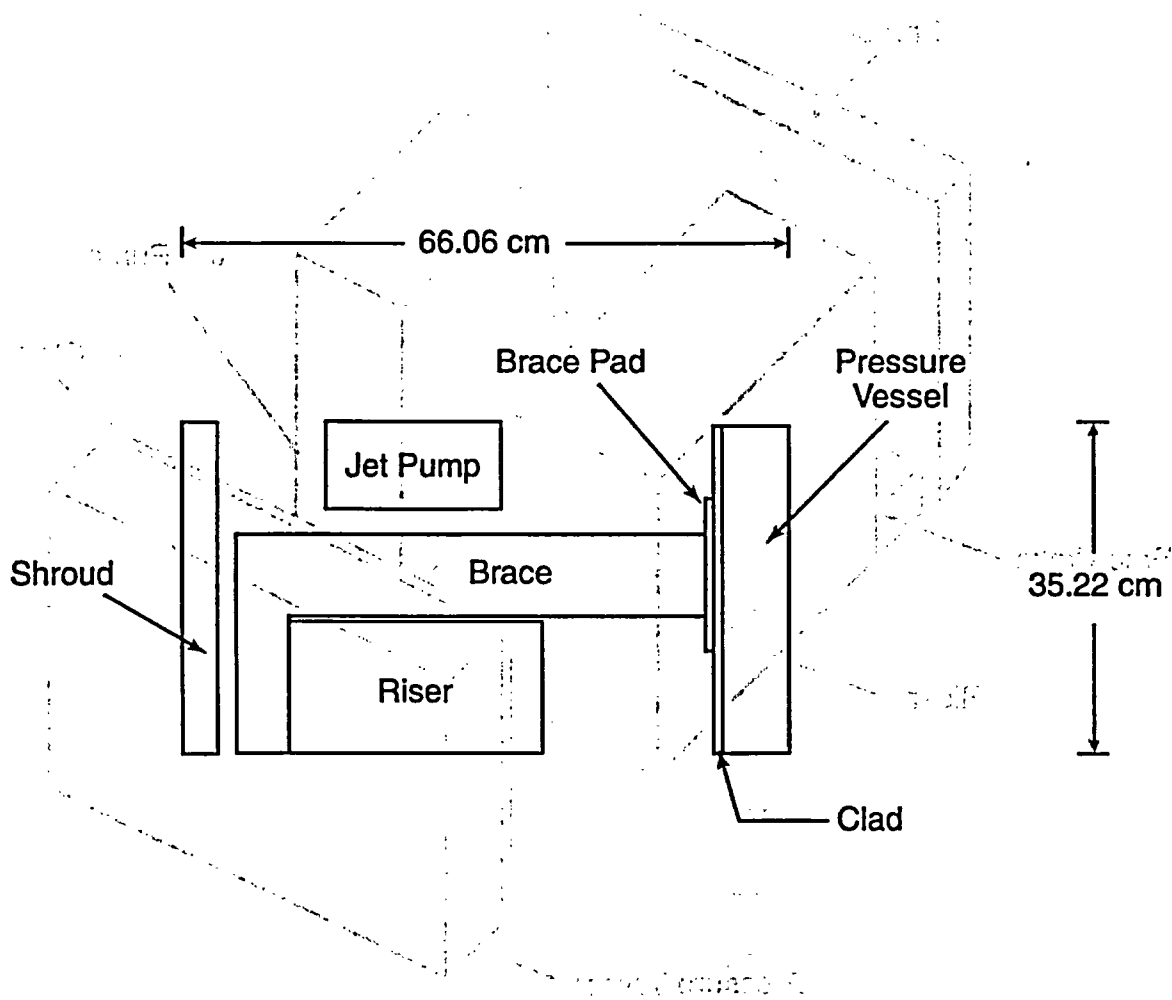


Figure 4.3. Top View of the Hatch-1 TORT Riser and Brace Model

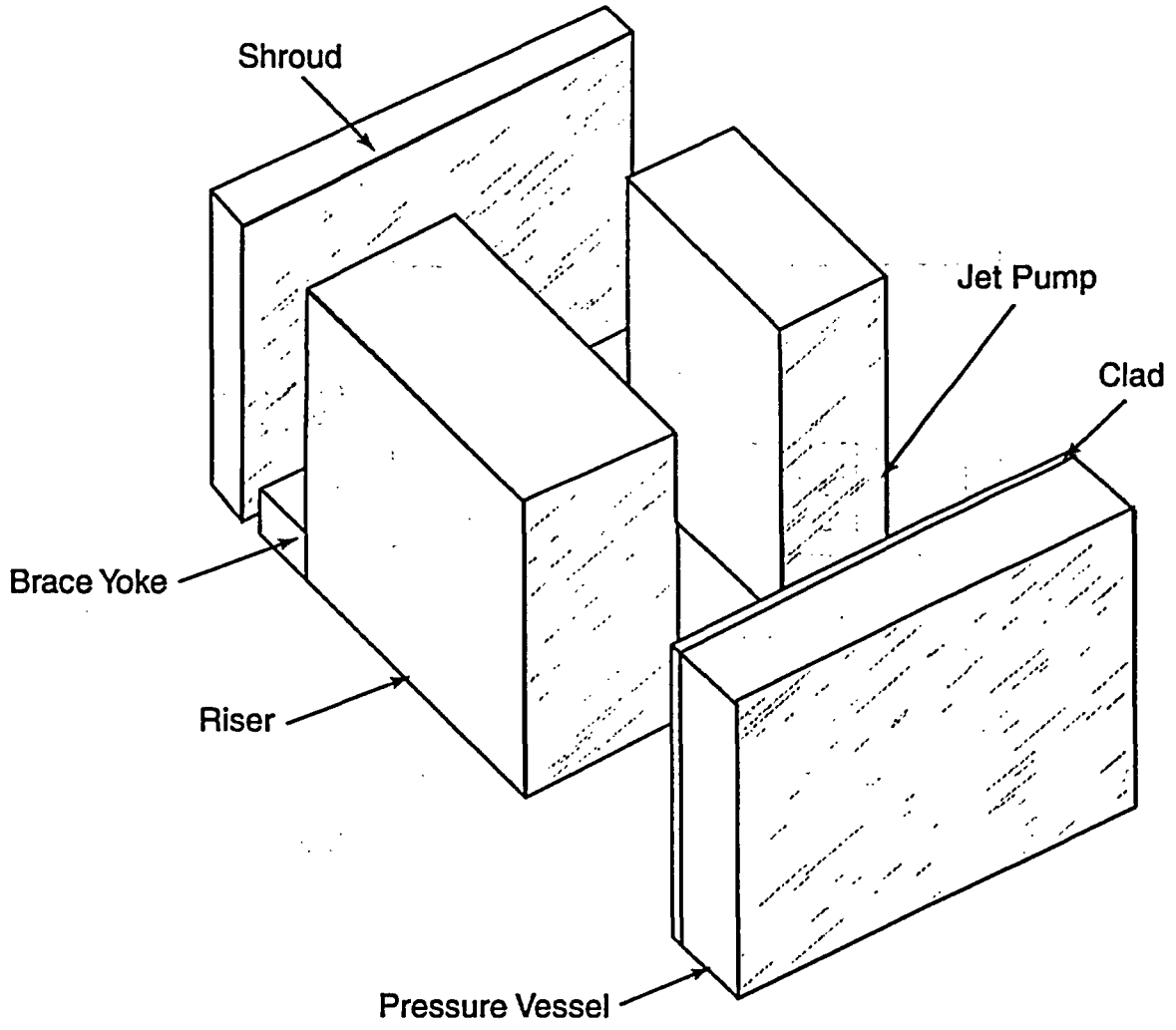


Figure 4.4. Side View of the Hatch-1 TORT Riser and Brace Model

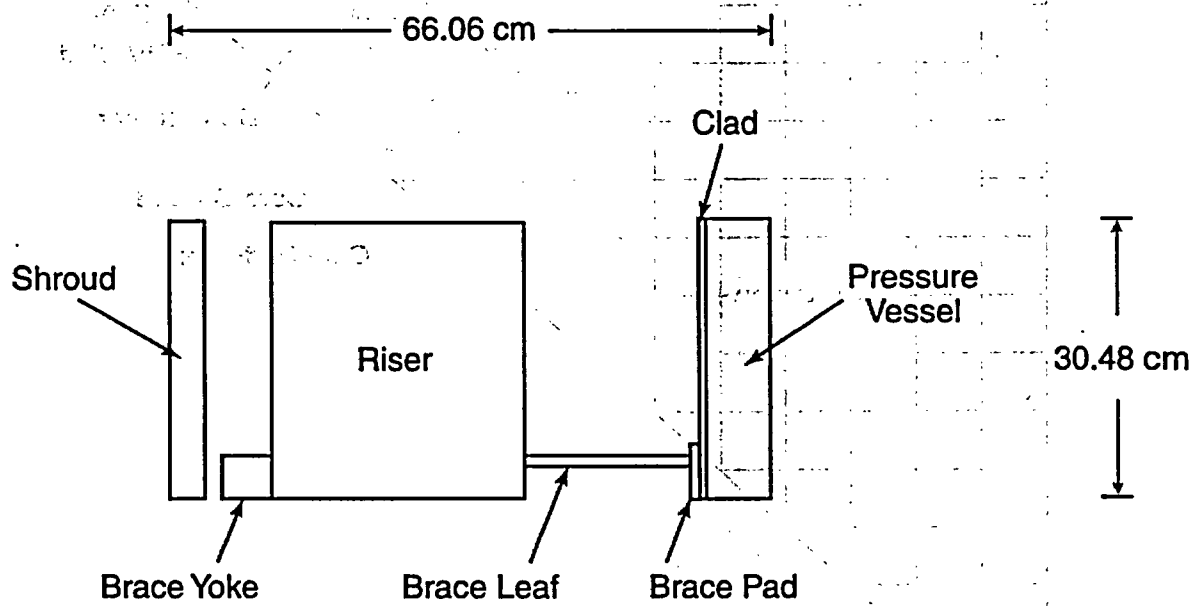


Figure 4.5. Horizontal View of the Hatch-1 TORT Riser and Brace Model

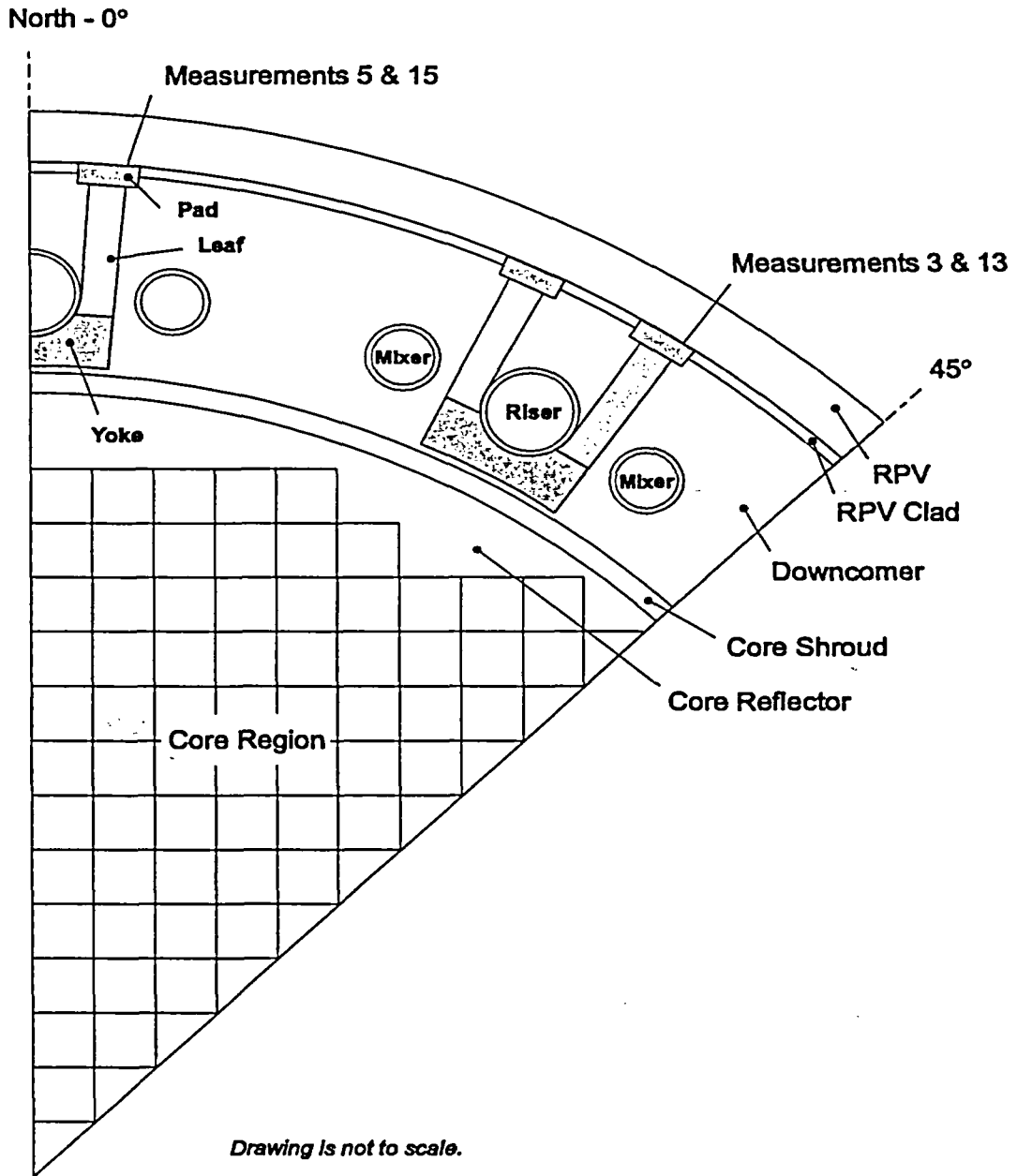
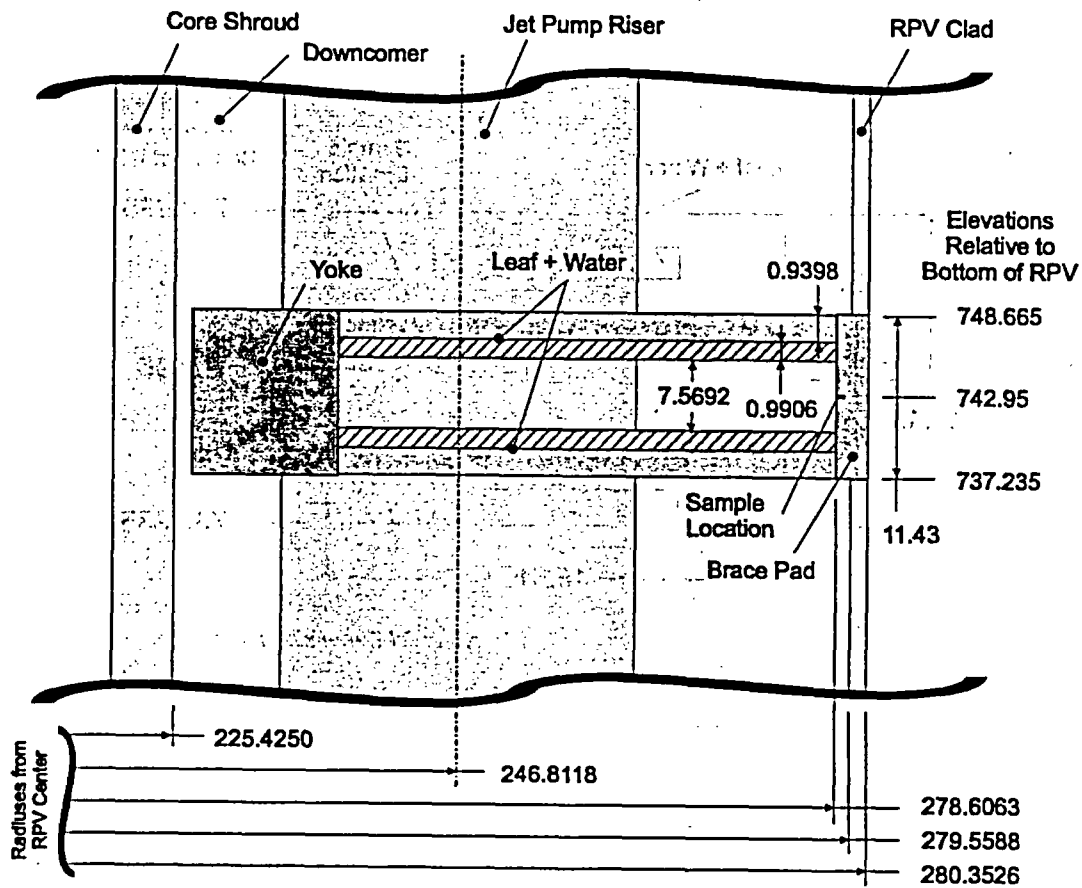


Figure 4.6. Top View of the Hatch-1 RAMA Model Near the Jet Pump Riser Brace Assembly Elevation



Note: All Dimensions In cm.

Figure 4.7. Axial View of the Hatch-1 RAMA Jet Pump Riser Brace Assembly Model

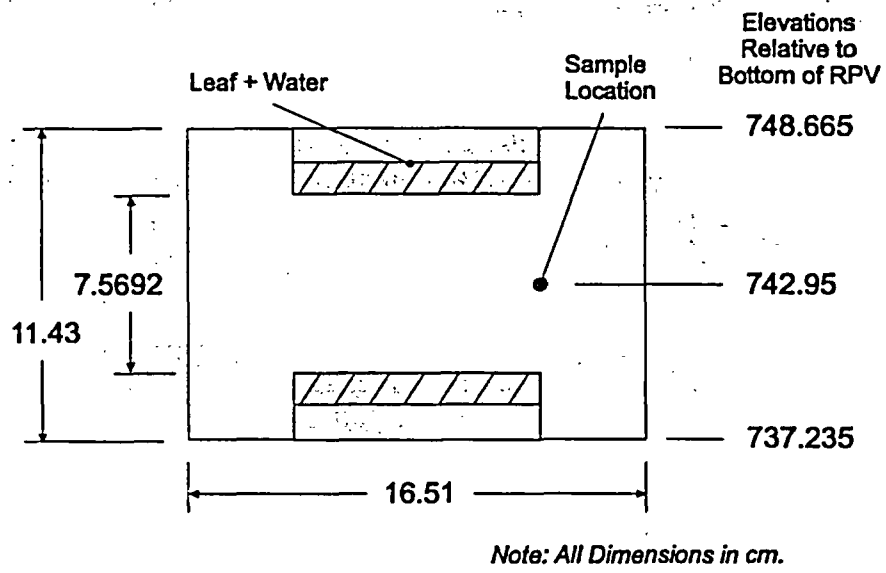


Figure 4.8. Front View of the Hatch-1 RAMA Jet Pump Riser Brace Pad

## 5 COMPARISONS OF CALCULATIONS AND MEASUREMENTS

### 5.1 Introduction

The Hatch-1 measurement program has provided a thermal and fast neutron dosimetry data-base for benchmarking BWR fluence calculation methodologies. Detailed calculations of the fast and thermal fluence of the brace pad scrapings have been performed using the DORT/TORT discrete ordinates transport methodology and the RAMA Fluence Methodology.

Comparisons of the DORT/TORT (performed by BNL) and RAMA (performed by TWE) predictions with the brace pad measurements were made to provide a direct assessment of the accuracy of the methodologies. In addition, comparisons of the DORT/TORT predictions with the RAMA methodology were made to provide a comparison of the two calculational methods. The RAMA methodology also calculates activities for irradiated specimens that are compared to measurements.

### 5.2 Brace Pad Dosimetry and Fluence Comparisons

The DORT/TORT and RAMA fluence predictions are compared with the measurements in Section 5.2.1 and the DORT/TORT to RAMA inter-code comparisons are presented in Section 5.2.2. Additional comparisons of RAMA predictions to activation measurements are presented in Section 5.2.3.

#### 5.2.1 Comparison of Fluence Calculations with Measurement

Before making the comparisons, it is first noted that the measurements corresponding to Jet Pump-3 and 13 are located at diametrically opposite locations on the vessel. Similarly, the locations of the Jet Pump 5 and 15 measurements are also diametrically opposed. Except for slight asymmetries ( $\leq 2\%$ ) resulting from core loading strategies, these symmetric measurements should be identical. However, a review of the Hatch-1 measurement data indicates that, while the symmetric locations generally indicate an asymmetry of  $\leq 9 \pm 2\%$ , the symmetrically located thermal measurements for Jet Pumps 3 and 13 differ by 30%. In addition, while the thermal-to-fast fluence ratios for the Jet Pump-13, 5 and 15 measurements are all in close agreement (to within

3%), the thermal-to-fast ratio for the Jet Pump-3 measurements differs by 20%. Consequently, the Jet Pump-3 measurement is considered unreliable and has been eliminated from the M/C comparisons. The Fe-58 (n,  $\gamma$ ) Fe-59 thermal data for the symmetric Jet Pump 5 and 15 measurements indicates a 30% asymmetry and has also been eliminated from the M/C comparisons.

The comparisons of the DORT/TORT calculations with the brace pad measurements are presented in Tables 5.2.1 and 5.2.2. The DORT/TORT calculations of the fast fluence (i.e.,  $>1$  MeV and  $>0.1$  MeV) are seen to agree with the eight measurements with an average measurement-to-calculation ratio of  $M/C = 0.97 \pm 0.08^3$ . The comparison of the DORT/TORT thermal fluence calculation and the three measurements gives an average M/C of  $1.17 \pm 0.07$ . The measured thermal values were reduced by 0.7% to make the adjusted measured value correspond to the group boundary used in the calculation, namely 0.414 eV. The 0.7% reduction factor was the calculated flux contribution (from 0.414 eV to 0.5 eV) compared to the calculated total thermal flux (from 0 to 0.5 eV). These M/C differences are within the estimated combined  $\sim 15\%$  DORT/TORT calculation uncertainty and  $\sim 10\text{-}15\%$  measurement uncertainty.

The RAMA calculations of the brace pad neutron dosimetry measurements are presented in Tables 5.2.3 and 5.2.4. The RAMA calculations of the fast fluences (i.e., energies  $>1$  MeV and  $>0.1$  MeV) agree with the measurements with an average measurement-to-calculation ratio of  $M/C = 0.93 \pm 0.04$ . Comparison of the RAMA thermal fluence calculation with the brace pad measurement indicates an average M/C of  $0.62 \pm 0.002$ . The M/C differences for the fast fluences are considered to be consistent with the estimated calculation and measurement uncertainties. The M/C differences for the thermal fluence is discussed in Section 5.2.3.

#### 5.2.2 Comparison of DORT/TORT and RAMA Fluence Results

The comparisons of the DORT/TORT and RAMA fluence predictions are compared with the measurements in Section 5.2.1 and the DORT/TORT to RAMA inter-code comparisons are presented in Section 5.2.2. Additional comparisons of RAMA predictions to activation measurements are presented in Section 5.2.3.

<sup>3</sup>All  $\pm$  differences are understood to be one-sigma values.



The comparisons of the DORT/TORT (BNL) and RAMA (TWE) fluence predictions of the Jet Pump-3/13 and Jet Pump-5/15 measurements are presented in Tables 5.2.5 and 5.2.6, respectively. The fast neutron fluence comparisons indicate an average code-to-code ratio of  $DORT/RAMA = 0.97 \pm 0.04$ . The thermal neutron fluence comparisons indicate an average code-to-code ratio of  $DORT/RAMA = 0.52 \pm 0.06$ . The fast fluence differences between the DORT/TORT and RAMA are within the estimated uncertainty of the two calculations.

The calculated thermal fluence comparisons for both methodologies do not show the consistency of the fast fluence predictions. Additional results edited from the RAMA methodology are presented in Section 5.2.3.

The DORT/TORT calculations showed smaller differences between the thermal fluence predictions and the thermal fluence measurements. The RAMA thermal fluence calculations showed larger differences in comparison to measurements. The DORT/TORT thermal fluence results were an under prediction of the fluence, while the RAMA results were an over prediction. Relative to the measurements, the DORT/TORT thermal fluences presented in Tables 5.2.1 and 5.2.2 were ~15% lower on average, and the TWE RAMA results presented in Tables 5.2.3 and 5.2.4 were ~60% higher on average.

### 5.2.3 Comparison of RAMA Activity Calculations with Measurements

The RAMA Fluence Methodology performs a three dimensional calculation that produces direct solutions (i.e., no multiplicative factors are used) for activations and neutron fluence. The comparisons of the RAMA calculated to measured activations are presented in Tables 5.2.7 - 5.2.9.

Table 5.2.7 shows comparisons of the symmetric Jet Pump-3 and 13 activation measurements to the RAMA calculated measurements. The average measurement to calculated (M/C) ratios for the fast activations is  $1.03 \pm 0.16$  and for the thermal activations is  $0.57 \pm 0.05$ . Similarly, Table 5.2.8 shows comparisons of the symmetric Jet Pump-5 and 15 activation measurements to the RAMA calculated measurements. The average M/C ratios for the fast activations is  $1.02 \pm 0.13$  and for the

thermal activations is  $0.59 \pm 0.05$ . Table 5.2.9 shows the averages for all measurement comparisons. The average M/C ratios for the fast activations is  $1.02 \pm 0.13$  and for the thermal activations is  $0.59 \pm 0.05$ . Measurement results for certain nuclides have been omitted from the comparisons (identified with an "n/a" in the tables) in accordance with discussions presented in Section 5.2.1. The niobium-93 meta-stable data provided in the BUGLE-96 data library has been determined to be unreliable and has also been omitted from the tables.

TWE believes the cause of the low M/C ratios for thermal activations could be attributable to the BUGLE-96 data library upon which the RAMA nuclear data library is based. The BUGLE-96 data has been derived for fast fluence predictions using spectra weighting and a group structure that may not be appropriate for the RAMA code's thermal predictions at the locations where the brace pad measurements were taken.

Table 5.2.1 - Comparison of the Jet Pump-3 and 13 Measured and DORT/TORT Calculated Fluences ( $\times 10^{-17}$  n/cm<sup>2</sup>).

Fluence Energy	Jet Pump-3 Measurement	Jet Pump-13 Measurement	Average Measurement	Calculated Fluence	Measurement/Calculation
E > 1-MeV	8.38	7.62	8.00	8.02	1.00
E > 0.1 MeV	15.8	14.3	15.1	14.1	1.07
E < 0.414 eV	NA	13.3	13.3	10.5	1.27

Table 5.2.2 - Comparison of the Jet Pump-5 and 15 Measured and DORT/TORT Calculated Fluences ( $\times 10^{-17}$  n/cm<sup>2</sup>).

Fluence Energy	Jet Pump-5 Measurement	Jet Pump-15 Measurement	Average Measurement	Calculated Fluence	Measurement/Calculation
E > 1-MeV	4.88	4.53	4.71	5.38	0.88
E > 0.1 MeV	9.10	8.47	8.79	9.48	0.93
E < 0.414 eV	7.99	7.88	7.93	7.06	1.12

Table 5.2.3 - Comparison of the Jet Pump-3 and 13 Measured and RAMA Calculated Fluences ( $\times 10^{-17}$  n/cm<sup>2</sup>).

Fluence Energy	Jet Pump-3 Measurement	Jet Pump-13 Measurement	Average Measurement	Calculated Fluence	Measurement/Calculation
E > 1-MeV	8.38	7.62	8.00	8.50	0.94
E > 0.1 MeV	15.8	14.3	15.1	15.3	0.98
E < 0.414 eV	NA	13.3	13.3	21.6	0.61

Table 5.2.4 - Comparison of the Jet Pump-5 and 15 Measured and RAMA Calculated Fluences ( $\times 10^{-17}$  n/cm<sup>2</sup>).

Fluence Energy	Jet Pump-5 Measurement	Jet Pump-15 Measurement	Average Measurement	Calculated Fluence	Measurement/Calculation
E > 1-MeV	4.88	4.53	4.71	5.29	0.89
E > 0.1 MeV	9.10	8.47	8.79	9.63	0.91
E < 0.414 eV	7.99	7.88	7.93	12.9	0.62

Table 5.2.5 - Comparison of the DORT/TORT and RAMA Predictions of the Jet Pump-3 and 13 Measurements ( $\times 10^{-17}$  n/cm<sup>2</sup>).

Fluence Energy	DORT/TORT Pump-3 and 13	RAMA Pump-3 and 13	Ratio DORT/TORT-to-RAMA
E > 1-MeV	8.02	8.50	0.94
E > 0.1 MeV	14.1	15.3	0.92
E < 0.414 eV	10.5	21.6	0.49

Table 5.2.6 - Comparison of the DORT/TORT and RAMA Predictions of the Jet Pump-5 and 15 Measurements ( $\times 10^{-17}$  n/cm<sup>2</sup>).

Fluence Energy	DORT/TORT Pump-5 and 15	RAMA Pump-5 and 15	Ratio DORT/TORT-to-RAMA
E > 1-MeV	5.38	5.29	1.02
E > 0.1 MeV	9.48	9.63	0.98
E < 0.414 eV	7.06	12.9	0.55

Table 5.2.7 - Comparison of Jet Pump-3 and 13 Activation Measurements ( $\mu\text{Ci}/\text{mg}$ ) to RAMA Calculated Activations

Product Nuclide	Jet Pump-3 Measurement	Jet Pump-13 Measurement	Average Measurement	Calculated Activation	Measurement/Calculation
<b>Thermal</b>					
Fe-55	n/a	7.34E-03	7.34E-03	1.15E-02	0.64
Ni-63	n/a	1.58E-02	1.58E-02	2.82E-02	0.56
Fe-59	n/a	1.14E-04	1.14E-04	1.82E-04	0.62
Cr-51	n/a	4.84E-02	4.84E-02	9.28E-02	0.52
Co-60	n/a	5.18E-03	5.18E-03	9.79E-03	0.53
				<b>Average</b>	<b>0.57</b>
				<b>Std. Dev.</b>	<b>0.05</b>
<b>Fast</b>					
Nb-93m	n/a	n/a	n/a	n/a	n/a
Mn-54	5.30E-04	5.59E-04	5.44E-04	4.69E-04	1.16
Co-58	4.71E-02	4.32E-02	4.52E-02	5.03E-02	0.90
				<b>Average</b>	<b>1.03</b>
				<b>Std. Dev.</b>	<b>0.16</b>

Table 5.2.8 - Comparison of Jet Pump-5 and 15 Activation Measurements ( $\mu\text{Ci}/\text{mg}$ ) to RAMA Calculated Activations

Product Nuclide	Jet Pump-5 Measurement	Jet Pump-15 Measurement	Average Measurement	Calculated Activation	Measurement/Calculation
<b>Thermal</b>					
Fe-55	4.48E-03	4.52E-03	4.50E-03	7.02E-03	0.64
Ni-63	9.11E-03	8.99E-03	9.05E-03	1.72E-02	0.52
Fe-59	n/a	n/a	n/a	n/a	n/a
Cr-51	2.90E-02	2.70E-02	2.80E-02	4.99E-02	0.54
Co-60	3.66E-03	3.54E-03	3.60E-03	5.74E-03	0.62
				<b>Average</b>	<b>0.59</b>
				<b>Std. Dev.</b>	<b>0.05</b>
<b>Fast</b>					
Nb-93m	n/a	n/a	n/a	n/a	n/a
Mn-54	3.11E-04	3.25E-04	3.18E-04	2.85E-04	1.12
Co-58	2.77E-02	2.68E-02	2.72E-02	2.98E-02	0.91
				<b>Average</b>	<b>1.02</b>
				<b>Std. Dev.</b>	<b>0.13</b>

Table 5.2.9 - Comparison of the Activation Measurements to RAMA Calculated Activities

Thermal Measurements (M/C)							Fast Measurements (M/C)			
Fe-55	Ni-63	Fe-59	Cr-51	Co-60	Average	Std. Dev.	Mn-54	Co-58	Average	Std. Dev.
.64	.54	.62	.54	.58	.59	0.05	1.14	0.90	1.02	0.13

## 6 SUMMARY AND CONCLUSION

In order to provide a benchmarking and assessment of BWR fluence calculation methods, detailed calculations of the Hatch-1 jet pump riser brace pad fast and thermal neutron dosimetry measurements have been performed using the DORT/TORT discrete ordinates transport methodology and the RAMA Fluence Methodology. The DORT/TORT and RAMA calculations have been compared with the measurements and with the predictions calculated with each methodology. Both measurement-to-code and code-to-code comparisons of the calculations have been performed to assess the accuracy of these methodologies for predicting the fast and thermal neutron fluence of BWR internal components and the vessel.

The calculations were performed using accepted (DORT/TORT) and state-of-the-art (RAMA) calculational methods together with the BUGLE-96 nuclear data library. The DORT/TORT and RAMA calculational models include a detailed description of the Hatch-1 core/internals/vessel material and geometrical configuration. The models include a cycle-by-cycle description of the Hatch-1 Cycle 1-19 operating history. The core neutron source includes the effects of the pin-wise power distribution on the core periphery and the effects of Pu buildup on the magnitude and energy dependence of the neutron source.

The DORT/TORT methodology (BNL) was found to predict the fast fluence measurements to within ~5% and the thermal fluence measurements to within ~15%. The observed agreement between the DORT/TORT calculation methodology and fluence measurements is generally considered to be consistent with the uncertainties in the calculations and measurements.

The RAMA fluence methodology was found to predict the fast fluence measurements to within ~7%. The RAMA thermal fluence predictions exceeded measured values by approximately 60%. Similar trends were observed in comparing fast and thermal activation predictions to measurements. That is, predicted fast activations were in much better agreement with measurements than were predicted thermal activations. While TWE currently believes that the differences in the thermal spectrum relative to the fast may be attributable to the derived BUGLE-96 thermal cross-section data used in the analysis, the reason for the differences requires further investigation.

The observed agreement for the fast fluence between the RAMA calculation methodology and measurements is generally considered to be consistent with the uncertainties in the calculations and measurements.

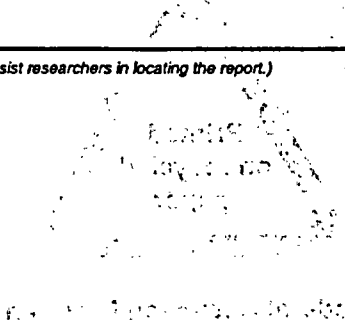
The DORT/TORT-to-RAMA differences for the fast fluence measurements are ~4%. The observed agreement between the fast fluence calculations and measurements and between the code predictions is generally considered to be consistent with the uncertainties in the calculations and measurements.

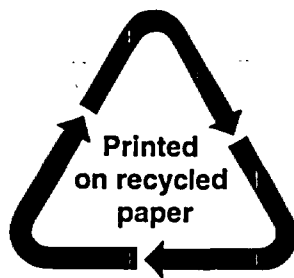
This report has described work performed under an Addendum to the NRC/EPRI Memorandum of Understanding (signed January 11, 2000) to remove and characterize samples from BWR in-vessel components. Under this cooperative agreement, each party was responsible for funding and administering certain activities. The NRC contracted BNL to perform work which included the following objectives: calculate fast and thermal fluences at the belt-line region of the core; compare the calculated values with fluences based on measurements; compare calculated BWR fluence results from a well-established computer code (DORT/TORT) with those from a newer, state-of-the-art, code (RAMA), and document the results. While the two codes were in good agreement for the prediction of fast fluence, there was a significant discrepancy in the thermal fluence predictions. With the completion of this report, the objectives of the BNL efforts have been accomplished. However, EPRI intends to initiate an activity later in 2004 to identify the source of the over-prediction of thermal fluence by RAMA.

## 7 REFERENCES

1. V. N. Shah and P. E. McDonald, eds., "Aging and Life Extension of Major Light Water Reactor Components," Elsevier Science Publishers B. V., Amsterdam, Netherlands, 1993.
2. Office of Nuclear Regulatory Research, "Calculational and Dosimetry Methods for Determining Pressure Vessel Neutron Fluence," Regulatory Guide 1.190, U.S. Nuclear Regulatory Commission, March 2001.
3. (a) L. R. Greenwood, "Retrospective Neutron Dosimetry for the Plant 1 Reactor," Attachment-A and "Retrospective Neutron Dosimetry for the Plant 2 Reactor," Attachment B to "Helium, Boron, and Radiometric Analysis of Reactor Steel-Plant-1, Project No. 40645 (JCN Y 6249)," Letter, B. M. Oliver (PNNL) to W. Norris (NRC), dated August 16, 2001.  
(b) "Calculations," Letter referring to Hatch-1, L. R. Greenwood (PNNL) to John Carew (BNL) dated October 15, 2002.
4. W. A. Rhoades et. al., "TORT-DORT Two- and Three-Dimensional Discrete Ordinates Transport, Version 2.8.14," CCC-543, Radiation Safety Information Computational Center, Oak Ridge National Laboratory, 1994.
5. D. B. Jones, K. E. Watkins and S. P. Baker, RAMA, Radiation Analysis Modeling Application, Proceedings PHYSOR 2000, ANS International Topical Meeting, Pittsburgh, PA, May 2000.
6. D. B. Jones and K. E. Watkins, "Fluence Evaluation of the Edwin I. Hatch-1BWR Plant Using the RAMA Transport Code," TransWare Enterprises Inc. (TWE) Interim Report, April 30, 2003.
7. "Plant Data Required for Hatch-1 Dosimetry Calculations," Letter, J. F. Carew (BNL) to K. Folk (Southern Company), dated July 30, 2001.
8. N. H. Larsen and J. G. Goudey, "Core Design and Operating Data for Cycle 1 of Hatch-1," Electric Power Research Institute Report EPRI NP-562, January 1979.
9. G. L. Holloway, J. E. Fawks and B. W. Crawford, "Core Design and Operating Data for Cycles 2 and 3 of Hatch-1," Electric Power Research Institute Report EPRI NP-2106, February 1984.
10. J. F. Carew, "Process Computer Performance Evaluation Accuracy," NEDO-20340, General Electric Company (1974).
11. "BUGLE-96: Coupled 47 Neutron, 20 Gamma-Ray Group Cross Section Library Derived from ENDF/B-VI for LWR Shielding and Pressure Vessel Dosimetry Applications," DLC-185, Radiation Safety Information Computational Center, Oak Ridge National Laboratory, July 1999.
12. "MESH - A Code for Determining the DOT Fixed Neutron Source," BNL-Memorandum, M. D. Zentner to J. F. Carew, August 25, 1981.
13. J. F. Carew, K. Hu, A. Aronson, A. Prince, and G. Zamonsky, "Pressure Vessel Fluence Calculation Benchmark Problems and Solutions," NUREG/CR-6115, BNL-NUREG-52395, September 2001.
14. "TRANSX 2.15: Code System to Produce Neutron, Photon, and Particle Transport Table for Discrete-Ordinates and Diffusion Codes from Cross Sections in MATXS Format", PSR-317, Radiation Safety Information Computational Center, Oak Ridge National Laboratory, June 1992.
15. "VITAMIN-B6: A Fine Group Cross Section Library Based on ENDF/B-VI Release 3 for Radiation Transport Applications", DLC-184, Radiation Safety Information Computational Center, Oak Ridge National Laboratory, 1996.



<b>NRC FORM 335</b> (9-2004) NRCMD 3.7		<b>U.S. NUCLEAR REGULATORY COMMISSION</b>		<b>1. REPORT NUMBER</b> (Assigned by NRC, Add Vol., Supp., Rev., and Addendum Numbers, If any.)  <b>NUREG/CR-6887</b>	
<b>BIBLIOGRAPHIC DATA SHEET</b> (See instructions on the reverse)					
<b>2. TITLE AND SUBTITLE</b> DORT/TORT Analyses of the Hatch Unit-1 Jet Pump Riser Brace Pad Neutron Dosimetry Measurements with Comparisons to Predictions Made with RAMA				<b>3. DATE REPORT PUBLISHED</b>	
				MONTH November	YEAR 2005
<b>5. AUTHOR(S)</b> J.F. Carew, K. Hu, A. Aronson, A.N. Mallen, and M. Todosow				<b>4. FIN OR GRANT NUMBER</b> Y6883	
				<b>6. TYPE OF REPORT</b> Technical	
<b>8. PERFORMING ORGANIZATION - NAME AND ADDRESS</b> (If NRC, provide Division, Office or Region, U.S. Nuclear Regulatory Commission, and mailing address; if contractor, provide name and mailing address.) Division of Engineering Office of Nuclear Regulatory Research U.S. Nuclear Regulatory Commission Washington, DC 20555-0001				<b>7. PERIOD COVERED</b> (Inclusive Dates) Sep 2003 - Jun 2004	
				<b>9. SPONSORING ORGANIZATION - NAME AND ADDRESS</b> (If NRC, type "Same as above"; if contractor, provide NRC Division, Office or Region, U.S. Nuclear Regulatory Commission, and mailing address.) same as above	
<b>10. SUPPLEMENTARY NOTES</b> W.E. Norris, NRC Project Manager					
<b>11. ABSTRACT</b> (200 words or less) <p>Detailed calculations of the Hatch-1 jet pump riser brace pad thermal and fast neutron dosimetry measurements have been performed by Brookhaven National Laboratory using the DORT/TORT discrete ordinates transport methodology and by Transware Enterprises, Inc., using the RAMA three-dimensional fluence methodology. The calculations were performed using a detailed description of the Hatch-1 core/internals/vessel material and geometrical configuration. Comparisons of the fluences calculated by DORT/TORT and fluences and activations calculated by RAMA and the Hatch-1 measurements were performed to assess the accuracy of the methodologies for predicting the fast and thermal neutron fluence of the BWR internal components and the vessel. Measurement-to-Calculation fluence comparisons were also performed. The core neutron source includes the effects of the pin-wise power distribution on the core periphery and the effects of plutonium buildup on the magnitude and energy dependence of the neutron source.</p>					
<b>12. KEY WORDS/DESCRIPTORS</b> (List words or phrases that will assist researchers in locating the report.) NUREG/CR-6887 fast neutron thermal neutron neutron dosimetry measurements BWR pressure vessel fluence fluence methodology DORT/TORT RAMA				<b>13. AVAILABILITY STATEMENT</b> unlimited	
				<b>14. SECURITY CLASSIFICATION</b> (This Page) unclassified (This Report) unclassified	
				<b>15. NUMBER OF PAGES</b> 60	
				<b>16. PRICE</b>	



**Federal Recycling Program**

NUREG/CR-6887

**DORT/TORT ANALYSES OF THE HATCH UNIT 1- JET PUMP RISER BRACE PAD  
NEUTRON DOSIMETRY MEASUREMENTS WITH  
COMPARISONS TO PREDICTIONS MADE WITH RAMA**

NOVEMBER 2005

**UNITED STATES  
NUCLEAR REGULATORY COMMISSION  
WASHINGTON, DC 20555-0001**

---

OFFICIAL BUSINESS